# Transient µm scale protein accumulation at the center of the T cell antigen presenting cell interface drives efficient IL-2 secretion

Danielle J. Clark [1], Laura E. McMillan [1], Clémentine Massoué [1], Lidiya Mykhaylechko [1], Xiongtao Ruan [2], Kentner L. Singleton [3], Minna Du [3], Alan J. Hedges [1], Pamela L. Schwartzberg [4], Robert F. Murphy [2,5,6], Christoph Wülfing [1,3]*

Danielle J. Clark and Laura E. McMillan contributed equally to this work

1 School of Cellular and Molecular Medicine, University of Bristol, Bristol BS8 1TD, United Kingdom
2 Computational Biology Department, School of Computer Science, Carnegie Mellon University, Pittsburgh, PA 15213, USA
3 Department of Immunology, University of Texas Southwestern Medical Center, Dallas, TX 75390, USA
4 Genetic Disease Research Branch, National Human Genome Research Institute, National Institutes of Health, Bethesda, MD 20892
5 Departments of Biological Sciences, Biomedical Engineering and Machine Learning, Carnegie Mellon University, Pittsburgh, PA 15213, USA
6 Freiburg Institute for Advanced Studies and Faculty of Biology, Albert Ludwig University of Freiburg, 79104 Freiburg, Germany
* email: Christoph.Wuelfing@bristol.ac.uk

**Abstract**

A μm scale complex, the central supramolecular signaling cluster (cSMAC), forms at the center of the interface of T cells activated by antigen presenting cells. It is of interest as μm scale protein complexes have unique biophysical and signaling properties. To causally determine cSMAC function, we have systematically manipulated the localization of three adaptor proteins, LAT, SLP-76, and Grb2. cSMAC recruitment varied between the adaptors and was consistently diminished upon blockade of the costimulatory receptor CD28 and deficiency of the signal amplifying kinase Itk. Reconstitution of adaptor cSMAC localization by fusion with domains with a strong interface localization preference restored IL-2 secretion as a key T cell effector function as dependent on the precise reconstitution dynamics. Our data establish a model where the cSMAC enhances early signaling by facilitating extensive signaling interactions and attenuates signaling thereafter through sequestration of a more limited set of signaling intermediates.

## Introduction

T cell activation is governed by substantial spatiotemporal organization of signal transduction across scales. At the nanoscale receptors form small clusters of dozens of molecules that can coalesce into microclusters and are commonly associated with active forms of signaling intermediates [1, 2, 3, 4, 5, 6]. This association strongly suggests that such receptor clusters play an important role in mediating efficient T cell signaling. Larger, μm scale assemblies were first described at the center and periphery of a T cell activated an by antigen presenting cells (APC) for the TCR, PKCθ and LFA-1, talin, respectively, as central and peripheral supramolecular activation clusters (cSMAC and pSMAC) [7, 8, 9]. The μm scale of assemblies, in particular in the form of supramolecular protein complexes, provides unique biophysical and signaling properties [10, 11, 12]. Supramolecular protein complexes play critical roles in viral sensing [13], the induction of inflammation [14], embryonic development [15], protein folding in cancer [16], nuclear ubiquitinylation [17], and chromatin compaction [18]. Such complexes are readily observed by fluorescence microscopy, held together by a network of multivalent protein interactions and often have distinct phase properties [10, 11, 12]. The cSMAC has many properties of such supramolecular protein complexes: It contains various multivalent signaling intermediates [19], prominently LAT (linker of activation of T cells), components of this complex including LAT and PKCθ exchange with the remainder of the cell to a moderate extent and slowly [20], and components of this complex can be assembled into supramolecular structures *in vitro* [21]. Therefore, understanding how the cSMAC regulates T cell activation is of substantial importance.

cSMAC function is controversial and unresolved despite decades of work. A central limitation in investigating the cSMAC is that its composition and/or assembly have not been systematically manipulated inside live T cells. Based on association of cSMAC formation with T cell activation conditions, the cSMAC has been proposed to enhance T cell signaling, terminate it, not be related to signaling or only upon weak stimulation or at late time points [8, 9, 22, 23, 24]. cSMAC formation is often associated with efficient T cell activation conditions, fitting with a role in enhancing T cell signaling. Accumulation of signaling intermediates at the T cell:APC interface center is substantially reduced by blockade of the critical costimulatory receptor CD28 [25, 26], in regulatory T cells [27], during thymic selection [28], or in the absence of the signal amplifying kinase Itk (IL-2 inducible T cell kinase) [29]. To causally investigate the function of μm scale protein accumulation at the T cell:APC interface center, we have systematically manipulated the localization of three adaptor proteins in live primary T cells: LAT [19] is an integral component of the cSMAC. SLP-76 (SH2 domain-containing leucocyte protein of 76 kD) [30] is associated with it only during the first minute of T cell activation [20]. Grb2 (growth factor receptor-bound 2) [31] association with the cSMAC is less prevalent [20]. Interface recruitment of all three adaptors was diminished upon attenuation of T cell activation by costimulation blockade and Itk-deficiency as was IL-2 secretion, a critical T cell effector function. We fused these adaptors with various protein domains with a strong interface localization preference to bring them back to the interface under the attenuated T cell activation conditions. Restoration of adaptor interface localization restored

diminished IL-2 secretion but only when executed to the extent and with the spatial features and dynamics seen under full stimulus conditions. The cSMAC thus enhanced T cell signaling and this ability depended on the careful tuning of its assembly.

## Results

### µm scale LAT accumulation at the center of the T cell APC interface was associated with efficient T cell activation

To causally investigate how µm scale protein accumulation at the center of the T cell:APC interface regulates T cell function, we first cataloged protein localization events that were consistently associated with efficient T cell function. To do so we attenuated T cell activation through costimulation blockade [25, 26] and Itk deficiency. Our model system [20, 25, 32] the 5C.C7 T cell receptor (TCR) recognizes the moth cytochrome C (MCC) 89-103 peptide presented by I-$E^k$. In the restimulation of *in vitro* primed 5C.C7 T cells with CH27 B cell lymphoma APCs and MCC peptide IL-2 amounts in the supernatant were reduced upon blockade of the CD28 ligands CD80 and CD86 with antibodies ('costimulation blockade') and in T cells from Itk knock out 5C.C7 TCR transgenic mice, in particular at lower peptide concentrations (Fig. 1A). Even at the highest MCC concentration of 10µM the amounts of T cell IL-2 mRNA were significantly ($p<0.001$) reduced to less than 50% upon costimulation blockade and Itk-deficiency (Fig. 1B).

Next, we characterized T cell signaling organization as extensively described before [20, 25, 32]. Briefly, 5C.C7 T cells are primed *in vitro* with APC and peptide, retrovirally transduced to express fluorescent signaling intermediates or sensors, FACS sorted to about 2µM sensor expression, as close as possible to endogenous signaling intermediate concentrations, and imaged in three dimensions over time during restimulation with APC and 10µM MCC peptide ('full stimulus'). In image analysis the frequency of occurrence of geometrically quantified µm scale subcellular distributions that represent underlying cell biological structures is determined (Supplementary Fig. 1A) [33]. Of particular interest here are accumulation at the center of the T cell APC interface ('central'), the cSMAC, and accumulation in a µm deep 'invagination' at the center of the interface that likely mediates termination of early central signaling [34]. 'Diffuse' accumulation mostly represents smaller areas of signaling clusters spread over the entire interface, possibly as a failed attempt to coalesce signaling into a larger central cluster. Upon costimulation blockade and Itk deficiency the frequency of central accumulation of signaling sensors was consistently diminished (Fig. 1C, D, Supplementary Figs. 1B-3, Supplementary Table 1) indicative of reduced cSMAC formation. These data establish that efficient IL-2 secretion is associated with µm scale central signaling localization.

LAT displayed µm scale central localization (Fig. 2A) in a biphasic pattern. At the time of tight cell coupling under full stimulus conditions 49±6% of cell couples showed central LAT accumulation. After 2min of cell coupling central LAT accumulation was reduced to about 25% of cell couples (Fig. 2B) and remained stable at that level. In the absence of Itk, the initial peak of central LAT accumulation was significantly ($p=0.005$) diminished to 26±6% of cell couples with central LAT accumulation. Such reduction was more pronounced (11±4%, $p<0.001$) upon costimulation blockade (Fig. 2B, Supplementary Table 2). Combining costimulation blockade and Itk deficiency yielded the least interface LAT accumulation (Fig. 2B). Impaired activation of cytoskeletal transport

processes is a likely contributor to diminished central LAT accumulation upon costimulation blockade and Itk deficiency, as enhancement of actin dynamics with active Rac and Cofilin [35] significantly ($p<0.001$, Fig. 2C, Supplementary Table 2)[35] increased central and overall LAT accumulation.

Reduced central LAT accumulation upon attenuation of T cell activation was associated with diminished LAT phosphorylation at Y191 (Fig. 2D, Supplementary Fig. 4) upon costimulation blockade, in particular in combination with Itk deficiency. At 2, 5, and 10 min after tight cell coupling LAT phosphorylation was significantly ($p\leq0.02$) reduced in Itk-deficient 5C.C7 T cells upon costimulation compared to wild type 5C.C7 T cells under full stimulus conditions at the same time point by 39%, 61%, and 70%, respectively. As central LAT localization was thus consistently associated with efficient T cell signaling and function we manipulated LAT localization to investigate how µm scale signaling localization at the interface center governs T cell function.

**Fusion of LAT with protein domains with pronounced interface localization preferences controlled LAT localization**

To systematically manipulate LAT localization, we added three protein domains with strong localization preference to LAT: PKCθ V3, Vav1 SH3SH2SH3, or PLCδ PH. The PKCθ V3 domain is required for central interface accumulation of PKCθ [36] even though it couldn't drive central localization by itself (Supplementary Fig. 5A). The Vav1 SH3SH2SH3 domains drove strong central accumulation only within the first minute of cell coupling (Supplementary Fig. 5A), as consistent with the localization of full length Vav1 (Supplementary Fig. 1B). The PLCδ PH domain mediated interface accumulation focused on the first two minutes of cell coupling without a central preference (Supplementary Fig. 5A).

Fusion of LAT to the PKCθ V3 domain (LAT V3) yielded efficient central accumulation that was well sustained over the entire imaging time frame under all conditions at levels around 50% of cell couples with central accumulation (Fig. 3). Starting 40s after tight cell coupling such sustained central accumulation was significantly ($p<0.05$, Supplementary Table 3) more frequent than central accumulation of non-targeted LAT under full stimulus at virtually every single time point. Fusion of LAT to the PKCθ V3 domain thus stabilized central LAT accumulation well beyond the levels seen for LAT alone under any physiological condition.

Fusion of LAT to the Vav1 SH3SH2SH3 domains ('LAT Vav') yielded different effects depending on the T cell activation conditions. Upon a full T cell stimulus LAT Vav resulted in diminished central and overall accumulation compared to LAT alone that was significant ($p<0.05$) across many time points (Fig. 3, Supplementary Table 3), suggesting that LAT Vav does not enhance properly assembled signaling distributions. Upon the three attenuated stimuli LAT Vav consistently enhanced central accumulation, most dramatically ($p\leq0.001$, at most time points) for costimulation blockade in wild type and Itk deficient cells (Fig. 3, Supplementary Table 3). LAT Vav accumulation upon attenuated T cell stimulation in any pattern was largely indistinguishable from non-targeted LAT

accumulation under full stimulus conditions ($p>0.05$, Supplementary Table 3) and central accumulation was moderately enhanced only between 1 and 3 minutes after tight cell coupling. Fusion of LAT to the Vav1 SH3SH2SH3 domain thus allowed for fairly close reconstitution of full stimulus-type LAT localization upon attenuated T cell stimulation.

Fusion of LAT to the PLCδ PH domain ('LAT PLCδPH') resembled LAT Vav but was less powerful. Upon full stimulation LAT PLCδPH significantly ($p<0.005$) diminished overall LAT interface accumulation within the first minute of cell coupling from >72% of cell couples with any interface accumulation to <52% (Fig. 3, Supplementary Table 3). Upon the three attenuated T cell stimuli LAT PLCδPH moderately enhanced central and overall LAT accumulation but didn't consistently reach the same extent as LAT alone under full stimulus conditions. For example in Itk-deficient 5C.C7 T cells upon costimulation blockade interface accumulation in any pattern was consistently enhanced ($p<0.005$ for time point 20 and later) from <32% to >55% upon expression of LAT PLCδPH. However, accumulation at the interface center only moderately increased from a range of 6-17% to 19-35%.

To ensure that overall interface accumulation of the targeted LAT constructs was comparable, we measured [32, 35] their interface recruitment upon costimulation blocked conditions. All constructs showed substantial interface recruitment with moderately less LAT Vav recruitment at the last four time points (Supplementary Fig. 5B, C). To ensure functionality of the targeted LAT constructs, we showed that they were tyrosine phosphorylated upon T cell activation (Supplementary Fig. 5D).

Fusion of LAT with protein domains with a strong interface localization preference thus allowed us to control LAT localization: Fusion with the PKCθ V3 domain yielded consistently enhanced central localization, fusion with the Vav1 SH3SH2SH3 domains largely restored full stimulus-type LAT localization upon costimulation blockade and Itk deficiency and fusion with the PLCδ PH domain resulted in partial restoration.

**Restoration of LAT centrality yielded enhanced IL-2 mRNA production**

To determine T cell function upon manipulation of LAT localization, we measured IL-2 mRNA induction upon 5C.C7 T cell activation with CH27 APCs and 10 μM MCC peptide, directly mirroring the imaging conditions. Expression of the targeting domains in isolation had only minor effects on IL-2 mRNA amounts (Supplementary Fig. 6). Forcing exaggerated central LAT localization by fusion with the PKCθ V3 domain did not affect IL-2 mRNA amounts (Fig. 4A, B). In contrast, restoring LAT centrality under costimulation blocked and Itk deficient conditions to slightly higher (LAT Vav) or slightly lower (LAT PLCδPH) levels than seen for non-targeted LAT under full stimulus conditions yielded a consistent and largely significant ($p<0.05$) increase in IL-2 mRNA (Fig. 4A, B) to levels close to the amounts of IL-2 mRNA in LAT-transduced 5C.C7 T cells under full stimulus conditions. For example, in LAT-expressing 5C.C7 T cells IL-2 mRNA amounts dropped to 18±6% and 18±3% of full stimulus mRNA upon costimulation blockade in wild type and Itk-deficient 5C.C7 T cells, respectively.

Expression of LAT Vav restored IL-2 mRNA to 41±9% and 58±10% ($p<0.01$), respectively, and expression of LAT PLCδPH to 50±9% ($p<0.05$) and 88±23%. µm scale central LAT interface accumulation thus supported efficient IL-2 secretion depending on its extent and dynamics.

**Forcing central LAT localization only modestly enhanced the central localization of related signaling intermediates**

Next, we investigated to which extent the forced relocalization of one signaling intermediate can drive analogous relocalization of others. We determined the subcellular distributions of Grb2, Lck and Vav1 in 5C.C7 T cells in the presence of LAT V3 using IRES-containing retroviral vectors for the parallel expression of GFP-tagged versions of the signaling intermediates alongside LAT V3. Under full stimulus conditions expression of LAT V3 moderately diminished interface recruitment of Grb2, Lck and Vav1, both in any pattern and at the center of the interface (Fig. 4C, Supplementary Table 4) suggesting that excessive central LAT localization upsets a finely balanced signaling system. Upon costimulation blockade the localization of all three signaling intermediates was largely unaffected by LAT V3. However, Grb2 and Lck centrality were moderately enhanced in the activation of Itk-deficient 5C.C7 T cells. For example, while the percentage of Itk-deficient 5C.C7 T cells with central Grb2-GFP expression did not exceed 7% at 40s after cell coupling and thereafter, upon co-expression of LAT V3 this percentage averaged 15% over the same time frame. The centrality of Vav1 as a signaling intermediate with only brief and moderate early central accumulation (Supplementary Fig. 1B) was not altered. The forced localization of LAT at the interface center thus could only draw in Grb2 and Lck as signaling intermediates with some intrinsic central localization preference to a modest extent and upon only one attenuated T cell stimulus.

**Restoration of SLP-76 centrality modestly enhanced IL-2 mRNA production**

To extend our understanding of the functional importance of µm scale protein accumulation at the interface center to a second signaling intermediate, we investigated SLP-76 as an adaptor with more transient central accumulation. At the time of tight cell coupling under full stimulus conditions 45±7% of the cell couples displayed SLP-76 accumulation at the interface center, similar to LAT. However, 80s later this percentage dropped to less than 10% (Fig. 5). Also similar to LAT, the peak of central SLP-76 accumulation was significantly ($p\leq0.01$) diminished upon costimulation blockade, Itk-deficiency and the combination of both to <27%, <15% and <11% of cell couples with central SLP-76 accumulation, respectively (Fig. 5B, Supplementary Table 5). To control SLP-76 localization, we fused it to the PKCθ V3 ('SLP-76 V3') or the Vav1 SH3SH2SH3 ('SLP-76 Vav') domain. Both constructs did not significantly affect SLP-76 centrality under full stimulus conditions, in wild type or Itk-deficient 5C.C7 T cells (Fig. 6A, Supplementary Table 6). However, accumulation of SLP-76 at the interface center was moderately but significantly ($p<0.05$ at at least two time points within the first minute of tight cell coupling, the peak of central SLP-76 accumulation) enhanced upon costimulation blockade in wild type and Itk-deficient 5C.C7 T cells reaching e.g. 67±7% and 33±7%, respectively, of cell couples with central SLP-76 accumulation upon expression of SLP-76 Vav (Fig. 6A, Supplementary Table 6). Interestingly, the enhancement of SLP-76 centrality

was limited to the first minute of tight cell coupling, the time where non-targeted SLP-76 accumulated at the interface center.

Consistent with the enhancement of SLP-76 centrality under costimulation-blocked conditions we observed a modest increase in IL-2 mRNA amounts under costimulation blocked conditions upon expression of SLP-76 V3 and SLP-76 Vav. Upon expression of non-targeted SLP-76 costimulation blockade in wild type and Itk-deficient 5C.C7 T cells reduced IL-2 mRNA amounts to 45±9% and 21±1%, respectively, of full stimulus (Fig. 6B). Expression of SLP-76 V3 restored IL-2 mRNA amounts to 87±20% and 74±24%, respectively, expression of SLP-76 Vav to 73±8% and 75±30% without reaching statistical significance in the stringent 2-way ANOVA (Fig. 6B). Upon restoration of central accumulation of the only transiently central signaling intermediate SLP-76 enhancement of IL-2 secretion was modest. Importantly, enhancement of centrality and IL-2 secretion remained closely linked across multiple T cell activation conditions and spatially targeted SLP-76 constructs (Fig. 4B) thus corroborating the importance of μm scale central protein accumulation for IL-2 secretion.

**PKCθ V3 and Vav1 SH3SH2SH3 didn't affect Grb2 centrality and IL-2 mRNA production**

To investigate the spatial features of forced interface recruitment of a signaling intermediate with more tentative central localization preference and their relation to IL-2 generation, we fused Grb2 2 to PKCθ V3 or Vav1 SH3SH2SH3. Upon 5C.C7 T cell activation with a full stimulus Grb2 is efficiently recruited to the T cell:APC interface during the first two minutes of tight cell coupling, peaking at 80±5% of cell couples with any interface accumulation. This overall interface accumulation was significantly ($p \leq 0.02$ at at least three time points within the first two minutes of tight cell coupling) diminished upon costimulation blockade, Itk-deficiency and both, remaining below 64%, 35% and 43%, respectively of cell couples with any interface accumulation (Fig. 7, Supplementary Table 7). Distinguishing Grb2 from LAT and SLP-76, Grb2 accumulation at the interface center didn't exceed 20% under any of the T cell activation conditions. Fusion of Grb2 with PKCθ V3 ('Grb2 V3') or Vav1 SH3SH2SH3 ('Grb2 Vav') did not enhance centrality under any of the T cell activation conditions (Fig. 8A, Supplementary Table 8). Fusion with the PKCθ V3 domain did not substantially alter Grb2 localization at all (Fig. 8). Fusion with the Vav1 SH3SH2SH3 domain enhanced overall Grb2 interface recruitment across many time points under all T cell activation conditions (Fig. 8). However, most of this accumulation was in the peripheral pattern, a pattern quite common with full length Vav1 (Supplementary Fig. 1B). As an important negative control, our targeting approach thus does not force proteins with a minor intrinsic central preference to the interface center. Expression of Grb2 V3 or Grb2 Vav did not alter IL-2 mRNA production under any of the T cell activation conditions (Fig. 8B) despite the substantially enhanced overall interface accumulation upon expression of Grb2 Vav. Overall Grb2 interface accumulation was not associated with the induction of efficient IL-2 mRNA production (Fig. 4B) in contrast to the μm scale central accumulation of LAT and SLP-76. These data thus provide an important specificity control for the functional importance of the central protein accumulation.

## Discussion

Our manipulation of the localization of proximal adaptor proteins in T cell activation provides insight into how proteins associate with and/or drive the formation of the µm scale cSMAC. Using a large scale live cell imaging approach we were able to distinguish between inefficient cSMAC formation and inefficient recruitment of a signaling intermediate to an existing cSMAC: As central interface accumulation of numerous signaling intermediates was consistently diminished upon costimulation blockade and Itk-deficiency (Fig. 1C, D) cSMAC formation was most likely impaired. µm scale central interface accumulation of spatially targeted LAT and SLP-76 upon the attenuated T cell stimuli thus has to represent cSMAC restoration. Whether lack of central Grb2 localization indicates lack of cSMAC formation or recruitment remains unresolved. In general, supramolecular complex formation becomes more likely with increasing concentrations and valences of the complex components [10, 11]. Accordingly, replacement of proline-rich regions in Sos that mediate multivalent LAT/Grb2/Sos interactions leads to reduced LAT clustering and phosphorylation [37]. Similarly, when LAT phosphorylation (Fig. 2C), as required for interactions of LAT with SH2 domain-containing signaling intermediates, was reduced upon costimulation blockade and Itk deficiency LAT clustering at the interface center was also diminished (Fig. 2 B). Compensation for such diminished LAT clustering by fusing LAT with additional protein localization domains restored µm scale central LAT accumulation. The dependence of LAT clustering on the number of functional protein interaction motifs, i.e. its valence, is consistent with a supramolecular protein complex nature of the cSMAC.

Supramolecular complexes can be driven by the polymerization of a single protein [13, 14, 17], can be built by molecularly defined interactions of a small number of proteins [10] or, likely most common, they can consists of an agglomeration of large numbers of proteins [16, 38], some of which may be membrane-bound [38]. While supramolecular complexes formed by a small number of components are often characterized by defined structures such as lipid droplets or fibers [12], our understanding of supramolecular complexes built from a large number of components is limited. LAT shares clustering at the interface center with a large number of other signaling intermediates (Fig.1)[20]. Moreover, as determined by fluorescence recovery after photobleaching close to half of the amount of three components of the central signaling complex, LAT, active Rac, and PKCθ, is immobile and the remainder exchanges only slowly with rest of the cell [20]. These data are consistent with the suggestion that the µm central signaling complex is compositionally complex and has partial solid state properties.

Interestingly, fusion domains could not drive spatial features of adaptor localization by themselves but could only enhance intrinsic adaptor localization preferences. We could enhance central LAT clustering across all time points, central SLP-76 clustering only during the first minute of cell coupling and central Grb2 clustering not at all. This is consistent with the accumulation patterns of the non-targeted adaptors under full stimulus conditions, sustained for LAT (Fig. 3), limited to the first minute for SLP-76 (Fig. 5), and inherently weaker for Grb2

(Fig. 7). Localization of the spatially targeted adaptors was driven by the combination of intrinsic localization motifs and the spatial information provided by the fused domains. In support, the specific localization preferences of the isolated targeting domains (Fig. S4A) were secondary in the context of their fusion to the adaptor proteins. While both PKCθ V3 and PLCδ PH did not display central localization in isolation, they enhanced central localization of LAT and SLP-76 (Figs. 3, 6). Thus formation of the cSMAC was driven by the additive interaction motifs of complex components with only secondary importance of the detailed biochemical nature of individual protein-protein interactions. This cooperativity is again consistent with a supramolecular protein complex nature of the cSMAC.

Based on the cooperative model of cSMAC formation it can be readily understood why artificially enhanced cSMAC formation did not lead to the recruitment of signaling intermediates with intrinsically weak cSMAC preference. LAT V3 excessively accumulated at the interface center (Fig. 3B). However, only central Grb2 and Lck accumulation was marginally enhanced in parallel and only in Itk-deficient T cells (Fig. 3C). Limited central accumulation of Vav1, Lck and Grb2 under full stimulus conditions in the absence of LAT V3 (Fig. 7, Supplementary Fig. 1B) establishes that the intrinsic motifs of these proteins for cSMAC association are weak. Providing a more stable cSMAC by expression of LAT V3 likely moderately increased the local concentrations of cSMAC components needed to recruit Vav1, Lck or Grb2, hence the moderately enhanced central accumulation of Grb2 and Lck, but couldn't overcome an intrinsic lack of valence for the efficient recruitment of these proteins to the cSMAC.

Reconstitution of central LAT and SLP-76 clustering under attenuated T cell activation conditions could restore IL-2 mRNA generation. The association of lack of Grb2 centrality with lack of an effect on IL-2 generation provides a specificity control. These data prove that μm scale central protein clustering is a critical component of efficient T cell signaling. In addition, the signal-enhancing role of the cSMAC depended on the specific extent and dynamics of its formation. For the cSMAC to enhance T cell function experimental reconstitution of cSMAC formation needed to closely mimic cSMAC features observed with non-targeted constructs under full stimulus conditions. Time-dependent roles of the cSMAC have been proposed before [24] yet are difficult to compare to the work here as the molecules investigated differed. In our work under full stimulus conditions LAT-GFP and SLP-76-GFP were efficiently recruited to the interface center within the first two minutes of T cell activation with diminished recruitment thereafter. Recruitment of LAT and SLP-76 to the interface center upon attenuation of T cell activation by fusion with the Vav1 SH3SH2SH3 and PLCδ PH domains closely reproduced these dynamics (Figs. 3B, 6) and largely restored IL-2 mRNA generation (Figs. 4A, 6). However, recruitment of LAT to the interface center to a greater extent and duration by fusion with PKCθ V3 (Fig. 3B) could not enhance IL-2 mRNA generation under any of the T cell activation conditions (Fig. 4A). We therefore suggest that the cSMAC displays two different time-dependent roles. Within the first one to two minutes of T cell activation it efficiently brings together the large number of proximal T cell signaling intermediates required for efficient T cell activation. Subsequently, a substantial number of key signalling

intermediates including SLP-76, Itk, PLCγ, and Vav1 leave the cSMAC and move to smaller signalling complexes supported by an interface-wide lamellal actin network [20]. Retention of a more limited subset of signalling intermediates in the cSMAC after this time thus may render them less accessible to their interaction partners and therefore diminish sustained signal transduction. Signal enhancing and attenuating roles of the cSMAC thus may both occur as regulated by the specific time-dependent composition of the complex.

Itk and costimulation likely contribute to cSMAC formation by overlapping yet partially distinct means. Recruitment to the interface center peaks within the first two minutes of cell coupling for both ligand-engaged CD28 [25, 39] and full length Itk [20]. Both thus can be expected to provide protein-protein interactions during the early signal amplifying stage of the cSMAC. Only Itk has enzymatic activity to directly modify cSMAC components. Curiously the Itk kinase domain is required to allow Itk to leave the cSMAC. In contrast to the transient cSMAC association of full length Itk the joint Itk recruitment domains without the kinase domain remain stably accumulated at the interface center [25]. These data could indicate kinase domain-dependent destabilizing interactions in the cSMAC or stabilization of smaller Itk-dependent signaling complexes in the actin-supported lamellum [20] to shift protein recruitment away from the cSMAC. Both costimulation and Itk regulate actin dynamics. However, while costimulation controls core actin turnover through the Arp2/3 complex and Cofilin [35], Itk only regulates a SLAT-dependent subset of actin dynamics [29]. CD28 thus can be expected to contribute more strongly to cSMAC directed transport in complex assembly [35](Fig. 2C).

## Acknowledgements

We acknowledge the University of Bristol FACS and Wolfson BioImaging facilities for providing equipment and technical support. The work was supported by grants from the US National Science Foundation (MCB1121793 to CW, MCB1121919 and MCB1616492 to RFM), ERC (CW: PCIG11-GA-2012-321554), BBSRC (CW: BB/P011578/1) and US National Institutes of Health (P41 GM103712).

## Author contributions

DJC, LEM, RFM, CW conceived the study and designed experiments, DJC, LEM, CM, LM, XR, KLS, MD, CW performed experiments and analyzed data, AJH executed statistical analysis, PLS provided Itk knock out mice, CW wrote the manuscript.

## Figure Captions

**Figure 1 CD28 and Itk regulate IL-2 secretion and signaling organization. A** 5C.C7 T cells, wild type or Itk-deficient ('Itk ko'), were reactivated by CH27 B cell APCs and the indicated concentration of MCC agonist peptide in the absence or presence of 10 μg/ml anti-CD80 plus anti-CD86 ('costimulation blockade'). IL-2 amounts in the supernatant as determined by ELISA are given relative to stimulation of wild type 5C.C7 T cells with 10 μM MCC with SEM. 4-8 experiments were averaged per condition. The statistical significance of differences as determined separately for each MCC peptide concentration by 1-way ANOVA is indicated. **B** Relative amounts of IL-2 mRNA as determined by qPCR are given upon 5C.C7 T cell activation similar to A with 10 μM as the lone MCC concentration. 3-18 experiments were averaged per condition. The statistical significance of differences as determined by 1-way ANOVA is indicated. **C** 5C.C7 T cells expressing the indicated sensors were activated by peptide loaded CH27 B cell APCs (10μM MCC) in the absence or presence of 10 μg/ml anti-CD80 plus anti-CD86 ('costimulation blockade') and percentage occurrence of each pattern of interface enrichment (Supplementary Fig. 1A) among all cell couples analyzed across multiple experiments is given in shades of red from -40 to 420 s. In addition, to address the rate of pattern change, the percentage change per 20-s interval was calculated (not shown). Cluster trees are given in pink. The source data for this figure panel and the sensors used are listed in Supplementary Table 1. **D** Similar to C the percentage of pattern occurrence is given for wild type and Itk-deficient ('Itk ko') 5C.C7 T cells activated with a full stimulus. Some of the wild type 5C.C7 full stimulus data are the same as in C.

**Figure 2 LAT localization and activation is regulated by costimulation and Itk. A** An interaction of a LAT-GFP-transduced 5C.C7 T cell with a CH27 B cell lymphoma APC (10 μM MCC peptide - full stimulus) is shown at the indicated time points (in minutes) relative to the time of formation of a tight cell couple. Differential interference contrast (DIC) images are shown in the top row, with top-down, maximum projections of 3-dimensional LAT-GFP fluorescence data in the bottom row. The LAT-GFP fluorescence intensities are displayed in a rainbow-like false-color scale (increasing from blue to red). The scale bar on the top left corresponds to 5μm. For display purposes, resolution in x and y is twice as high as in all other imaging data. A video covering the entire time frame is available as Supplementary video S1. **B** The graphs display the percentage of cell couples with LAT accumulation in the indicated patterns (Supplementary Fig. 1A) relative to tight cell couple formation for wild type or Itk-deficient 5C.C7 T cells activated with CH27 B cell APCs (10 μM MCC peptide) in the absence or presence of 10 μg/ml anti-CD80 plus anti-CD86 ('costimulation blockade') as indicated. 47-77 cell couples were analyzed per condition, 226 total. A statistical analysis is given in Supplementary Table 2. **C** Itk-deficient 5C.C7 T cells were activated with CH27 B cell APCs (10 μM MCC peptide) in the presence of 10 μg/ml anti-CD80 plus anti-CD86 and 250 nM constitutively active Cofilin plus 1 μM constitutively active Rac1 as protein transduction reagents. LAT interface accumulation is given as in B. 30 cell couples were analyzed. The statistical significance of differences in LAT accumulation compared to Itk-deficiency plus

costimulation blockade is given in Supplementary Table 2. **D** 5C.C7 T cells were activated as in B. At the indicated time points T cell:APC cell extracts were blotted for LAT phosphorylation at Y191. Band intensities as normalized to the 1 min time point under full stimulus conditions are given. 5-7 experiments were averaged per condition. The statistical significance of differences as determined separately for each time point by 1-way ANOVA is indicated.

**Figure 3 LAT localization can be controlled by fusion with protein domains with a strong interface localization preference. A** A schematic representation of LAT-GFP is given (top) with LAT accumulation data under full stimulus conditions (bottom, from Fig. 2B) as a reference for the rest of the figure. **B** On top schematic representations are given for the three fusion proteins of LAT with protein domains with a strong intrinsic localization preference as indicated. Corresponding imaging data are given in the respective columns below in a standardized format: wild type or Itk-deficient 5C.C7 T cells transduced to express the spatially targeted LAT construct indicated on the top of the column were activated with CH27 B cell APCs (10 μM MCC peptide) in the absence or presence of 10 μg/ml anti-CD80 plus anti-CD86 ('costimulation blockade') with different T cell activation conditions given in separate rows as indicated. Each individual graph gives the percentage of cell couples that displayed accumulation of the spatially targeted LAT construct with the indicated patterns (Supplementary Fig. 1A) relative to tight cell couple formation in solid colors. Broken grey and red lines indicate accumulation of non-targeted LAT-GFP in any or the central interface pattern, respectively, under the same T cell activation conditions (from Fig. 2B) to demonstrate how fusion with protein domains with a strong intrinsic localization preference alters LAT localization. For costimulation blocked conditions representative imaging data are given similar to Fig. 2A. Videos covering the entire time frames are available as Supplementary videos S2-4. 37-53 cell couples were analyzed per condition, 551 total. Statistical analysis is given in Supplementary Table 3.

**Figure 4 Restoration of LAT centrality enhances IL-2 generation upon Itk deficiency and costimulation blockade but only modestly affects centrality of other signaling intermediates. A** Wild type or Itk-deficient ('Itk ko') 5C.C7 T cells were transduced to express LAT-GFP or a spatially targeted variant thereof as indicated and reactivated by CH27 APCs (10 μM MCC peptide) in the absence or presence of 10 μg/ml anti-CD80 plus anti-CD86 ('costimulation blockade'). IL-2 mRNA amounts are given relative to IL-2 mRNA in non-transduced 5C.C7 T cells under full stimulus conditions. 3-9 experiments were averaged per condition. Statistical significance of differences across all conditions as determined by 2-way ANOVA is given in the table on the right. **B** Sensor accumulation at the interface center and IL-2 mRNA amounts are summarized for all signaling intermediates, all spatially targeted variants thereof under all T cell activation conditions as indicated. Traces are the percentage cell couples with central accumulation from Figs. 3, 6, 8. Red color indicates enhanced central accumulation relative to non-targeted signaling intermediate under full stimulus conditions at at least half of the time points with substantial central accumulation, blue color similarly indicates diminished central accumulation. Four shades of grey indicated level of IL-2 mRNA relative to non-targeted

signaling intermediate under full stimulus conditions in 25% increments, i.e. >75%, 50-75%, 25-50% and <25%. **C** Wild type and Itk-deficient 5C.C7 T cells were transduced to express LAT V3 together with the indicated GFP-tagged signaling intermediate and activated with CH27 B cell APCs (10 μM MCC peptide) in the absence or presence of 10 μg/ml anti-CD80 plus anti-CD86 ('costimulation blockade') with different T cell activation conditions given in separate rows as indicated. Each individual graph gives the percentage of cell couples that displayed accumulation of the GFP-tagged signaling intermediate with the indicated patterns (Supplementary Fig. 1A) relative to tight cell couple formation in solid colors. Broken grey and red lines indicate accumulation of the signaling intermediate in the absence of LAT V3 in any or the central interface pattern, respectively, under the same T cell activation conditions (from Fig. 7, Supplementary Figs. 1B-3). 30-56 cell couples were analyzed per condition, 373 total. Statistical analysis is given in Supplementary Table 4.

**Fig. 5 SLP-76 localization is regulated by costimulation and Itk. A** An interaction of a SLP-76-GFP-transduced 5C.C7 T cell with a CH27 B cell APC (10 μM MCC peptide - full stimulus) is shown at the indicated time points (in minutes) relative to the time of formation of a tight cell couple as in Fig. 2A. A video covering the entire time frame is available as Supplementary video S5. **B** The graphs display the percentage of cell couples with SLP-76 accumulation in the indicated patterns (Supplementary Fig. 1A) relative to tight cell couple formation for wild type or Itk-deficient 5C.C7 T cells activated with CH27 B cell APCs (10 μM MCC peptide) in the absence or presence of 10 μg/ml anti-CD80 plus anti-CD86 ('costimulation blockade') as indicated. 47-83 cell couples were analyzed per condition, 231 total. A statistical analysis is given in Supplementary Table 5.

**Figure 6 SLP-76 localization can be controlled by fusion with protein domains with a strong interface localization preference. A** On top schematic representations are given for SLP-76-GFP and the two fusion proteins of SLP-76 with protein domains with a strong intrinsic localization preference as indicated. Corresponding imaging data are given in the respective columns below in a standardized format: wild type or Itk-deficient 5C.C7 T cells transduced to express the spatially targeted SLP-76 construct indicated on the top of the column were activated with CH27 B cell APCs (10 μM MCC peptide) in the absence or presence of 10 μg/ml anti-CD80 plus anti-CD86 ('costimulation blockade') with different T cell activation conditions given in separate rows as indicated. Each individual graph gives the percentage of cell couples that displayed accumulation of the non-targeted (on the left for reference) or spatially targeted SLP-76 construct (middle and right) with the indicated patterns (Supplementary Fig. 1A) relative to tight cell couple formation in solid colors. Broken grey and red lines indicate accumulation of non-targeted SLP-76-GFP in any or the central interface pattern, respectively, under the same T cell activation conditions (from Fig. 5B). For costimulation blocked conditions representative imaging data are given in addition on the middle left similar to Fig. 2A. Videos covering the entire time frames are available as Supplementary videos S6, 7. 39-52 cell couples were analyzed per condition, 355 total. Statistical analysis is given in Supplementary Table 6. **B** Wild type or Itk-deficient ('Itk ko')

5C.C7 T cells were transduced to express SLP-76-GFP or a spatially targeted variant thereof as indicated and reactivated by CH27 B cell APCs (10 μM MCC peptide) in the absence or presence of 10 μg/ml anti-CD80 plus anti-CD86 ('costimulation blockade'). IL-2 mRNA amounts are given relative to IL-2 mRNA in non-transduced 5C.C7 T cells under full stimulus conditions. 2-8 experiments were averaged per condition. Statistical significance of differences across all conditions as determined by 2-way ANOVA is given on the right.

**Fig. 7 Grb2 localization is regulated by costimulation and Itk. A** An interaction of a Grb2-GFP-transduced 5C.C7 T cell with a CH27 B cell APC (10 μM MCC peptide - full stimulus) is shown at the indicated time points (in minutes) relative to the time of formation of a tight cell couple as in Fig. 2A. A video covering the entire time frame is available as Supplementary video S8. **B** The graphs display the percentage of cell couples with Grb2 accumulation in the indicated patterns (Supplementary Fig. 1A) relative to tight cell couple formation for wild type or Itk-deficient 5C.C7 T cells activated with CH27 B cell APCs (10 μM MCC peptide) in the absence or presence of 10 μg/ml anti-CD80 plus anti-CD86 ('costimulation blockade') as indicated. 42-59 cell couples were analyzed per condition, 204 total. A statistical analysis is given in Supplementary Table 7.

**Figure 8 Grb2 localization can be controlled by fusion with protein domains with a strong interface localization preference. A** On top schematic representations are given for Grb2-GFP and the two fusion proteins of Grb2 with protein domains with a strong intrinsic localization preference as indicated. Corresponding imaging data are given in the respective columns below in a standardized format: wild type or Itk-deficient 5C.C7 T cells transduced to express the spatially targeted Grb2 construct indicated on the top of the column were activated with CH27 B cell APCs (10 μM MCC peptide) in the absence or presence of 10 μg/ml anti-CD80 plus anti-CD86 ('costimulation blockade') with different T cell activation conditions given in separate rows as indicated. Each individual graph gives the percentage of cell couples that displayed accumulation of the non-targeted (on the left for reference) or spatially targeted Grb2 construct (middle and right) with the indicated patterns (Supplementary Fig. 1A) relative to tight cell couple formation in solid colors. Broken grey and red lines indicate accumulation of non-targeted Grb2-GFP in any or the central interface pattern, respectively, under the same T cell activation conditions (from Fig. 7B). For costimulation blocked conditions representative imaging data are given in addition on the middle left similar to Fig. 2A. Videos covering the entire time frames are available as Supplementary videos S9, 10. 41-62 cell couples were analyzed per condition, 387 total. Statistical analysis is given in Supplementary Table 8. **B** Wild type or Itk-deficient ('Itk ko') 5C.C7 T cells were transduced to express Grb2-GFP or a spatially targeted variant thereof as indicated and reactivated by CH27 B cell APCs (10 μM MCC peptide) in the absence or presence of 10 μg/ml anti-CD80 plus anti-CD86 ('costimulation blockade'). IL-2 mRNA amounts are given relative to IL-2 mRNA in non-transduced 5C.C7 T cells under full stimulus conditions. 2-5 experiments were averaged per condition. Statistical significance of differences across all conditions as determined by 2-way ANOVA is given on the right.

## Methods

### Antibodies and reagents

Antibody used for quantitative Western blotting were α-LAT pY191 (Cell Signaling, #3584), α-GAPDH Clone 14C10 (Cell Signaling, #2118), and α-alpha Tubulin Clone DM1A (ThermoFisher Scientific, #62204). Antibodies used for the blockade of B7-1- and B7-2-dependent CD28 costimulation were anti-mouse CD80 Clone 16-10-A1 (BD Pharmingen #553736) and anti-CD86 Clone GL1 (BD Pharmingen #553689). Protein transduction versions of constitutively active cofilin (S3A) and Rac1 (Q61L) were purified from *E. coli* and introduced into primary 5C.C7 T cells by 30min incubation as previously described [35].

### Mice and cells

Itk-deficient 5C.C7 mice were generated by crossing B10.BR 5C.C7 TCR transgenic mice [40] with Itk-deficient B6 mice [41]. T cells expanded from the lymph nodes of wild type or Itk-deficient 5C.C7 TCR transgenic mice were used for all experiments. The 5C.C7 TCR recognizes the moth cytochrome c peptide fragment (amino acid residues 88 to 103, ANERADLIAYLKQATK) in the context of I-$E^k$. Single-cell suspensions were made from the lymph nodes of 6- to 8-week-old mice of either gender. The cells were adjusted to 4 x $10^6$ cells/ml and MCC peptide was added to a final concentration of 3 μM. T cells were transduced with MMLV-derived retroviruses for the expression of signaling sensors, commonly signaling intermediates fused with GFP as described in detail [20, 25, 32]. All animals were maintained in pathogen-free animal facilities at the University of Bristol under a University mouse breeding Home Office License. The CH27 B cell lymphoma cell line was used in all experiments as APCs. To load the APCs, the cells were incubated in the presence of 10 μM MCC peptide for at least 4 hours. All cells were maintained in medium composed of RPMI with L-glutamine, 10% fetal bovine serum (FBS, Hyclone), penicillin (100 IU/mL), streptomycin (100 μg/ml), and 0.5μM β-mercaptoethanol. Interleukin-2 (IL-2) was added at a final concentration of 0.05 U/ml during parts of the retroviral transduction procedure.

### Time-lapsed imaging of T cell:APC interactions

Our imaging and image analysis protocols have recently been described in great detail in a dedicated publication [32]. Briefly, time-lapse fluorescence microscopy was performed with retrovirally transduced T cells, FACS-sorted to the lowest detectable sensor expression of 2 μM, and CH27 cells loaded with 10μM MCC. The T cells and CH27 cells were imaged in imaging buffer (PBS, 10% FBS, 1 mM $CaCl_2$, 0.5 mM $MgCl_2$) on 384-well glass-bottom plates. All imaging was performed on a Perkin Elmer UltraVIEW ERS 6FE spinning disk confocal systems fitted onto a Leica DM I6000 microscope body equipped with full environmental control and a Hamamatsu C9100-50 EMCCD. A Leica 40x HCX PL APO oil objective (NA=1.25) was used for all imaging. Automated control of the microscope was performed with Volocity software (Perkin Elmer). For experiments in which the B7-1- and B7-2-dependent activation of CD28 was blocked, peptide-loaded CH27 cells were incubated on ice for 30 min in the presence of anti- CD80 Clone 16-10-A1 (10 μg/ml) and anti- CD86 Clone GL1 (10 μg/ml)(BD Pharmingen) antibody before the CH27 cells were transferred to the

imaging plate with the T cells. For experiments in which cells were reconstituted with protein transduction versions of constitutively active Rac and cofilin, T cells were incubated for 30 min at 37°C with the protein transduction reagents at the indicated concentrations in the imaging plate before the addition of the peptide-loaded CH27 cells. Each time-lapse image sequence was generated by taking a differential interference contrast brightfield image and a 3D image stack of the GFP channel every 20 s for 46 frames at 37°C. Voxels in these 3D images were of size 0.34 μm in the horizontal plane and 1 μm along the optical axis.

**Image Analysis**

The location and frame number of each T cell:APC couple were identified as when either the T cell:APC interface had reached its full width or the cells had been in contact for 40 s, whichever came first. Patterns of signaling sensor enrichment were assessed according to previously established quantitative criteria (Fig. 2 in [25]) as depicted in the Supplementary Figure 1A. Briefly, the six, mutually exclusive interface patterns were: accumulation at the center of the T cell-APC interface (central), accumulation in a large T cell invagination (invagination), accumulation that covered the cell cortex across central and peripheral regions (diffuse), accumulation in a broad interface lamellum (lamellum), accumulation at the periphery of the interface (peripheral) or in smaller protrusions (asymmetric). Briefly, for each cell couple at each time point we first determined whether fluorescence intensity in the area of accumulation was >40% above the cellular fluorescence background. If so, the geometrical features of the area of accumulation, fraction of the interface covered, location within the interface, and extension of the area of accumulation away from the interface (Fig. 2 in [25]), were used to assign the cell couple to one of the mutually exclusive patterns. Systems-scale cluster analysis was performed with Cluster (Michael Eisen, UC Berkeley) as established [25].

To measure interface enrichment of LAT and spatially targeted versions thereof we used a recently developed computational image analysis routine [35]. Very briefly, starting with the manual cell couple identification described above T cells were segmented, reoriented with the T cell:APC interface facing up using the 'two-point synapse annotation' procedure [35], and the cell shape was standardized to a half spheroid to allow voxel-by-voxel comparison across all cell couples analysed. After transformation to the standard shape, the fluorescence distribution in each cell at a given time point was represented as a standardized vector (of length 6628) formed from the intensity values of each of the voxels within the template shape, where the intensities for each time point were normalized so that the values of the vector were probabilities (that is, fractions of total intensity). To measure interface enrichment, we defined an interface enrichment region as the 10% most fluorescent voxels of the average probability distribution across all cells, for all time points, and for all sensors. We defined enrichment to be the ratio of the mean probability in the distribution of that sensor for that cell at that time point within the interface enrichment region and the mean probability in the entire cell.

**IL-2 ELISA**

Live wild type or Itk-deficient 5C.C7 T cells were FACS sorted to generate comparable cell numbers across each assay. CH27 B cells were peptide loaded

with 10μM MCC for four hours or overnight. T and B cells were mixed in round bottom 96-well plates at $1x10^4$ T cells to $5x10^4$ B cells. For costimulation blockade 10μg/ml α-CD80 and α-CD86 were added to each well. The cells were then incubated for 18 hours and IL-2 amounts in the supernatant were determined using a mouse IL-2 OptEIA ELISA kit from BD Biosciences as per manufacturer's instructions.

**IL-2 mRNA determination**

CH27 B cell lymphoma APCs were peptide loaded overnight with 10μM MCC peptide. Live wild type or Itk-deficient 5C.C7 T cells, non-transduced or expressing adaptor protein-GFP or targeted variants thereof, were FACS sorted to generate comparable cell numbers across each assay. $1x10^4$ T cells and $5x10^4$ APCs cells were centrifuged for 30 seconds at 1,000rpm to maximize cell-to-cell contact and incubated at 37°C for 2 hours. For costimulation blockade 10μg/ml α-CD80 and α-CD86 were added to each well. mRNA was isolated using the Qiagen RNeasy Micro Kit (Qiagen, UK) according to manufacturer's instructions. cDNA was generated using an Invitrogen AMV First-Strand cDNA synthesis kit (Life Technologies, UK) according to manufacturer's instructions. IL-2 mRNA amounts were determined with a SYBR Green PCR master mix from Life Technologies (4344463) relative to mRNA for β-2 microglobulin on a DNA Engine Opticon II System (Bio-Rad) using the following oligonucleotides, IL-2: AGCTGTTGATGGACCTA and CGC AGA GGT CCA AGT TCA T, β-2 microglobulin: GCTATCCAGAAAACCCCTCAA and CGG GTG GAA CTG TGT GTT ACG T.

**Western blotting analysis**

CH27 B cell lymphoma APCs were peptide loaded overnight with 10μM MCC peptide. Live wild type or Itk-deficient 5C.C7 T cells, non-transduced or expressing LAT-GFP or a targeted variant thereof, were FACS sorted to generate comparable cell numbers across each assay. $1x10^6$ T cells and $1x10^6$ APCs cells were centrifuged for 30 seconds at 1,000rpm to maximize cell-to-cell contact and incubated at 37°C for the indicated time. Subsequently, samples were immediately lysed with cold RIPA lysis buffer (Millipore) plus protease/ phosphatase inhibitor cocktail (Cell Signaling) for 30 minutes on ice. To remove the insoluble fraction, samples were centrifuged at 20,000g for 15 minutes. Supernatant were run on SDS/PAGE gels, transferred to PDVF membranes and blotted according to standard protocols. Blots were stripped and reprobed with an anti-GAPDH or anti-α tubulin antibody to normalize for sample loading.

**Statistics**

The frequency of occurrence of interface accumulation patterns was analyzed pairwise with a proportion's z-test as reported in the supplementary tables. p values were not corrected for multiple comparisons as the corresponding pFDR q-values [42] were similar. IL-2 mRNA amounts were first logarithmically transformed to stabilize the variance and approximate to the normal distribution and then analyzed by 1-way ANOVA with Tukey's adjustment for multiple comparisons or 2-way ANOVA with the Sidak adjustment for multiple comparisons depending on the number of variables compared. IL-2 ELISA data were first logarithmically transformed and then analyzed by 1-way ANOVA with Tukey's adjustment for multiple comparisons. LAT phosphorylation data were

first logarithmically transformed and then analyzed by 1-way ANOVA with Tukey's adjustment for multiple comparisons separately for each time point.

**Data availability statement**

All imaging data are openly accessible through http://murphylab.cbd.cmu.edu/data/TcellLAT2018/
IL-2 and LAT phosphorylation data that support the findings of this study are available from the corresponding author upon reasonable request.

**Supplementary Table 1 Sensors used in Fig. 1C, D.** Publications describing the sensors used in Fig. 1C, D and representative 5C.C7 T cell imaging data are given.

**Supplementary Table 2 Statistical significance of differences in LAT accumulation under different T cell activation conditions** are given for the indicated patterns as determined by proportion's z-test. No entry indicates p>0.05.

**Supplementary Table 3 Statistical significance of differences in accumulation of spatially targeted as compared to non-targeted LAT under different T cell activation conditions** are given for the indicated patterns as determined by proportion's z-test. No entry indicates p>0.05.

**Supplementary Table 4 Statistical significance of differences in accumulation of Grb2, Lck and Vav1 in the presence as compared to absence of LATV3 under different T cell activation conditions** are given for the indicated patterns as determined by proportion's z-test. No entry indicates p>0.05.

**Supplementary Table 5 Statistical significance of differences in SLP-76 accumulation under different T cell activation conditions** are given for the indicated patterns as determined by proportion's z-test. No entry indicates p>0.05.

**Supplementary Table 6 Statistical significance of differences in accumulation of spatially targeted as compared to non-targeted SLP-76 under different T cell activation conditions** are given for the indicated patterns as determined by proportion's z-test. No entry indicates p>0.05.

**Supplementary Table 7 Statistical significance of differences in Grb2 accumulation under different T cell activation conditions** are given for the indicated patterns as determined by proportion's z-test. No entry indicates p>0.05.

**Supplementary Table 8 Statistical significance of differences in accumulation of spatially targeted as compared to non-targeted Grb2 under different T cell activation conditions** are given for the indicated patterns as determined by proportion's z-test. No entry indicates p>0.05.

**Supplementary Fig. 1 Sensor accumulation at the T cell:APC interface under full stimulus conditions. A** The panel graphically represents the six categories used to classify spatiotemporal features of sensor accumulation at the T cell:APC interface as defined in detail previously [25, 33]. The antigen-presenting cell above the T cell is not shown. For all main figures the patterns 'diffuse' and 'lamellal' are combined as 'diffuse/lamellal', the patterns 'asymmetric' and 'peripheral' as 'periphery'. **B** The graphs display the percentage of cell couples that displayed accumulation of the indicated sensor (Supplementary Table 1) with the indicated patterns (A) relative to tight cell couple formation for wild type 5C.C7 T cells activated with CH27 B cell APCs (10 μM MCC peptide). 49-141

cell couples were analyzed per condition, 869 total.

**Supplementary Fig. 2 Sensor accumulation at the T cell:APC interface under costimulation blocked conditions.** The graphs display the percentage of cell couples that displayed accumulation of the indicated sensor (Supplementary Table 1) with the indicated patterns (Supplementary Fig. 1A) relative to tight cell couple formation for wild type 5C.C7 T cells activated with CH27 B cell APCs (10 μM MCC peptide) in the presence of 10 μg/ml anti-CD80 plus anti-CD86. 39-107 cell couples were analyzed per condition, 869 total.

**Supplementary Fig. 3 Sensor accumulation at the T cell:APC interface in the absence of Itk.** The graphs display the percentage of cell couples that displayed accumulation of the indicated sensor (Supplementary Table 1) with the indicated patterns (Fig. S1A) relative to tight cell couple formation for Itk-deficient 5C.C7 T cells activated with CH27 B cell APCs (10 μM MCC peptide). 30-67 cell couples were analyzed per condition, 582 total.

**Supplementary Fig. 4 Representative phosphor-LAT Y191 Western blot.** Wild type or Itk-deficient 5C.C7 T cells were activated with CH27 B cell and 10 μm MCC in the presence or absence of 10 μg/ml anti-CD80 plus anti-CD86. At the given time points (in minutes) T cell:APC cell extracts were blotted for LAT phosphorylation at Y191. Blots were stripped and reblotted with an anti-alpha tubulin antibody as a loading control. Phospho-LAT Y191 band intensities as normalized to loading control are given under the phospho-LAT blots. Molecular weights of marker bands (in kD) are given at the right. One representative blot of eight is shown.

**Supplementary Fig. 5 Patterning of isolated targeting domains and interface recruitment of LAT-GFP and spatially targeted version thereof. A** The graphs give the percentage of cell couples that displayed accumulation of the isolated targeting domains, LAT V3, LAT Vav, and LAT PLCδPH as indicated, with the indicated patterns (Supplementary Fig. 1A) relative to tight cell couple formation for wild type 5C.C7 T cells activated with CH27 B cell APCs (10 μM MCC peptide). 30-57 cell couples were analyzed per condition, 133 total. **B, C** For the quantification of the accumulation of LAT and targeted versions thereof at the T cell:APC interface we applied a computational image quantification as recently described in detail [35]. We identified a core region (B) of sensor enrichment as defined as the 10% most fluorescent voxels of the average probability distribution across all cells, for all time points, and for all sensors. Using this core region we calculated the ratio of the amount of the sensor in the region to the average amount across the whole cell. This was done for all time points either under conditions of full stimulus or costimulation blockade as indicated. Imaging data analyzed are the same as in Figs. 2 and 3. **D** Wild type 5C.C7 T cells retrovirally transduced to express the indicated LAT constructs were activated with CH27 B cell APCs and 10 μm MCC in the presence of 10 μg/ml anti-CD80 plus anti-CD86. At the given time points T cell:APC cell extracts were blotted for LAT phosphorylation at Y191. Blots were stripped and reblotted with an anti-alpha tubulin antibody as a loading control. One representative blot of two is shown.

**Supplementary Fig. 6 IL2 mRNA amounts upon expression of the isolated targeting domains.** Wild type or Itk-deficient ('Itk ko') 5C.C7 T cells were transduced to express the isolated targeting domains, LAT V3, LAT Vav, and LAT PLCδPH as indicated, and reactivated by CH27 APCs (10 μM MCC peptide) in the absence or presence of 10 μg/ml anti-CD80 plus anti-CD86 ('costimulation blockade'). IL-2 mRNA amounts are given relative to IL-2 mRNA in non-transduced 5C.C7 T cells under full stimulus conditions. 3-6 experiments were averaged per condition. None of the differences were significant as calculated with 2-way ANOVA.

**Supplementary video 1.** Representative interactions of 5C.C7 T cells retrovirally transduced to express the indicated GFP fusion proteins with CH27 B cell lymphoma APCs and 10 μM MCC peptide in the presence or absence of 10 μg/ml anti-CD80 plus anti-CD86 ('costimulation blockade') are shown in Supplementary videos S1 to S10. DIC images are shown on the top, with matching top-down, maximum projections of 3D sensor fluorescence data on the bottom. The sensor fluorescence intensity is displayed in a rainbow-like, false-color scale (increasing from blue to red). 20 s intervals in video acquisition are played back as 2 frames per second. The 5C.C7 T cell in Video S1 is transduced with LAT-GFP and responds to a full stimulus. Cell coupling occurs in frame 4 (2s indicated video time).

**Supplementary video S2.** The video is displayed similar to Video S1. The 5C.C7 T cell in Video S2 is transduced with LAT V3-GFP and responds to a full stimulus upon costimulation blockade. Cell coupling occurs in frame 4 (2s indicated video time).

**Supplementary video S3.** The video is displayed similar to Video S1. The 5C.C7 T cell in Video S3 is transduced with LAT Vav-GFP and responds to a full stimulus upon costimulation blockade. Cell coupling occurs in frame 5 (2s indicated video time).

**Supplementary video S4.** The video is displayed similar to Video S1. The 5C.C7 T cell in Video S4 is transduced with LAT PLCδ PH-GFP and responds to a full stimulus upon costimulation blockade. Cell coupling occurs in frame 5 (2s indicated video time).

**Supplementary video S5.** The video is displayed similar to Video S1. The 5C.C7 T cell in Video S5 is transduced with SLP-76-GFP and responds to a full stimulus. Cell coupling occurs in frame 4 (2s indicated video time).

**Supplementary video S6.** The video is displayed similar to Video S1. The 5C.C7 T cell in Video S6 is transduced with SLP-76 V3-GFP and responds to a full stimulus upon costimulation blockade. Cell coupling occurs in frame 4 (2s indicated video time).

**Supplementary video S7.** The video is displayed similar to Video S1. The 5C.C7 T cell in Video S7 is transduced with SLP-76 Vav-GFP and responds to a full stimulus upon costimulation blockade. Cell coupling occurs in frame 5 (2s

indicated video time).

**Supplementary video S8.** The video is displayed similar to Video S1. The 5C.C7 T cell in Video S8 is transduced with Grb2-GFP and responds to a full stimulus. Cell coupling occurs in frame 5 (2s indicated video time).

**Supplementary video S9.** The video is displayed similar to Video S1. The 5C.C7 T cell in Video S9 is transduced with Grb2 V3-GFP and responds to a full stimulus upon costimulation blockade. Cell coupling occurs in frame 4 (2s indicated video time).

**Supplementary video S10.** The video is displayed similar to Video S1. The 5C.C7 T cell in Video S10 is transduced with Grb2 Vav-GFP and responds to a full stimulus upon costimulation blockade. Cell coupling occurs in frame 5 (2s indicated video time). A second T cell activates at the left edge of the filed in frame 7 (3s indicated video time).


1. Hu YS, Cang H, Lillemeier BF. Superresolution imaging reveals nanometer- and micrometer-scale spatial distributions of T-cell receptors in lymph nodes. *Proc Natl Acad Sci U S A* **113,** 7201-7206 (2016).

2. Varma R, Campi G, Yokosuka T, Saito T, Dustin ML. T cell receptor-proximal signals are sustained in peripheral microclusters and terminated in the central supramolecular activation cluster. *Immunity* **25,** 117-127 (2006).

3. Yokosuka T*, et al.* Newly generated T cell receptor microclusters initiate and sustain T cell activation by recruitment of Zap70 and SLP-76. *Nat Immunol* **6,** 1253-1262 (2005).

4. Sherman E*, et al.* Functional nanoscale organization of signaling molecules downstream of the T cell antigen receptor. *Immunity* **35,** 705-720 (2011).

5. Boyle S*, et al.* Quantum dot fluorescence characterizes the nanoscale organization of T cell receptors for antigen. *Biophys J* **101,** L57-59 (2011).

6. Lillemeier BF, Pfeiffer JR, Surviladze Z, Wilson BS, Davis MM. Plasma membrane-associated proteins are clustered into islands attached to the cytoskeleton. *Proc Natl Acad Sci U S A* **103,** 18992-18997 (2006).

7. Monks CR, Freiberg BA, Kupfer H, Sciaky N, Kupfer A. Three-dimensional segregation of supramolecular activation clusters in T cells. *Nature* **395,** 82-86 (1998).

8. Monks CR, Kupfer H, Tamir I, Barlow A, Kupfer A. Selective modulation of protein kinase C-theta during T-cell activation. *Nature* **385,** 83-86 (1997).

9. Grakoui A, *et al.* The immunological synapse: A molecular machinery controlling T cell activation. *Science* **285,** 221-226 (1999).

10. Li P, *et al.* Phase transitions in the assembly of multivalent signalling proteins. *Nature* **483,** 336-340 (2012).

11. Banani SF, *et al.* Compositional Control of Phase-Separated Cellular Bodies. *Cell* **166,** 651-663 (2016).

12. Shin Y, Brangwynne CP. Liquid phase condensation in cell physiology and disease. *Science* **357,** (2017).

13. Cai X, *et al.* Prion-like polymerization underlies signal transduction in antiviral immune defense and inflammasome activation. *Cell* **156,** 1207-1222 (2014).

14. Franklin BS, *et al.* The adaptor ASC has extracellular and 'prionoid' activities that propagate inflammation. *Nat Immunol* **15,** 727-737 (2014).

15. Brangwynne CP, *et al.* Germline P granules are liquid droplets that localize by controlled dissolution/condensation. *Science* **324,** 1729-1732 (2009).

16. Rodina A, *et al.* The epichaperome is an integrated chaperome network that facilitates tumour survival. *Nature* **538,** 397-401 (2016).

17. Marzahn MR, *et al.* Higher-order oligomerization promotes localization of SPOP to liquid nuclear speckles. *EMBO J* **35,** 1254-1275 (2016).

18. Larson AG, *et al.* Liquid droplet formation by HP1alpha suggests a role for phase separation in heterochromatin. *Nature* **547,** 236-240 (2017).

19. Balagopalan L, Kortum RL, Coussens NP, Barr VA, Samelson LE. The linker for activation of T cells (LAT) signaling hub: from signaling complexes to microclusters. *J Biol Chem* **290,** 26422-26429 (2015).

20. Roybal KT, *et al.* Early Signaling in Primary T Cells Activated by Antigen Presenting Cells Is Associated with a Deep and Transient Lamellal Actin Network. *PLoS One* **10,** e0133299 (2015).

21. Su X, *et al.* Phase separation of signaling molecules promotes T cell receptor signal transduction. *Science* **352,** 595-599 (2016).

22. Cemerski S*, et al.* The balance between T cell receptor signaling and degradation at the center of the immunological synapse is determined by antigen quality. *Immunity* **29,** 414-422 (2008).

23. Lee KH*, et al.* T cell receptor signaling precedes immunological synapse formation. *Science* **295,** 1539-1542. (2002).

24. Freiberg BA*, et al.* Staging and resetting T cell activation in SMACs. *Nat Immunol* **3,** 911-917 (2002).

25. Singleton KL*, et al.* Spatiotemporal patterning during T cell activation is highly diverse. *Sci Signal* **2,** ra15 (2009).

26. Wülfing C*, et al.* Costimulation and endogenous MHC ligands contribute to T cell recognition. *Nat Immunol* **3,** 42-47 (2002).

27. Zanin-Zhorov A*, et al.* Protein kinase C-theta mediates negative feedback on regulatory T cell function. *Science* **328,** 372-376 (2010).

28. Ebert PJ, Ehrlich LI, Davis MM. Low ligand requirement for deletion and lack of synapses in positive selection enforce the gauntlet of thymic T cell maturation. *Immunity* **29,** 734-745 (2008).

29. Singleton KL*, et al.* Itk controls the spatiotemporal organization of T cell activation. *Sci Signal* **4,** ra66 (2011).

30. Koretzky GA, Abtahian F, Silverman MA. SLP76 and SLP65: complex regulation of signalling in lymphocytes and beyond. *Nat Rev Immunol* **6,** 67-78 (2006).

31. Jang IK, Zhang J, Gu H. Grb2, a simple adapter with complex roles in lymphocyte development, function, and signaling. *Immunol Rev* **232,** 150-159 (2009).

32. Ambler R, Ruan X, Murphy RF, Wulfing C. Systems Imaging of the Immune Synapse. *Methods Mol Biol* **1584,** 409-421 (2017).

33. Roybal KT, Sinai P, Verkade P, Murphy RF, Wülfing C. The actin-driven spatiotemporal organization of T-cell signaling at the system scale. *Immunol Rev* **256,** 133-147 (2013).

34. Singleton KL*, et al.* A large T cell invagination with CD2 enrichment resets receptor engagement in the immunological synapse. *J Immunol* **177,** 4402-4413 (2006).

35. Roybal KT*, et al.* Computational spatiotemporal analysis identifies WAVE2 and cofilin as joint regulators of costimulation-mediated T cell actin dynamics. *Sci Signal* **9,** rs3 (2016).

36. Kong KF*, et al.* A motif in the V3 domain of the kinase PKC-theta determines its localization in the immunological synapse and functions in T cells via association with CD28. *Nature immunology* **12,** 1105-1112 (2011).

37. Kortum RL*, et al.* The ability of Sos1 to oligomerize the adaptor protein LAT is separable from its guanine nucleotide exchange activity in vivo. *Sci Signal* **6,** ra99 (2013).

38. Tarantino N*, et al.* TNF and IL-1 exhibit distinct ubiquitin requirements for inducing NEMO-IKK supramolecular structures. *J Cell Biol* **204,** 231-245 (2014).

39. Purtic B, Pitcher LA, van Oers NS, Wülfing C. T cell receptor (TCR) clustering in the immunological synapse integrates TCR and costimulatory signaling in selected T cells. *Proc Natl Acad Sci USA* **102,** 2904-2909 (2005).

40. Seder RA, Paul WE, Davis MM, Fazekas de St. Groth B. The presence of interleukin 4 during in vitro priming determines the lymphokine-producing potential of CD4+ T cells from T cell receptor transgenic mice. *J Exp Med* **176,** 1091-1098 (1992).

41. Schaeffer EM*, et al.* Requirement for Tec kinases Rlk and Itk in T cell receptor signaling and immunity. *Science* **284,** 638-641 (1999).

42. Storey JB. Strong control, conservative point estimation adn simultaneous conservative consistency of false discovery rates: a unified approach. *J R Statist Soc B* **66,** 187-205 (2004).

**Table S1**

| Signaling intermediate | Sensor | Location of classification data/representative video |
|---|---|---|
| Actin | GFP-Actin | JI 2003 |
| Akt | Akt-GFP | PLoS One 2015 |
| Arp3 | Arp3-GFP | Sci Signal. 2016 |
| Capping protein 1 $\alpha$ | Capping protein 1 $\alpha$-GFP | Sci Signal. 2016 |
| CD2 | CD48-GFP | Sci Signal. 2009 |
| Cdc42 | WASP GBD-GFP-CAAX | Sci Signal. 2009 |
| Cofilin | Cofilin-GFP | Sci Signal. 2016 |
| Coronin 1A | Coronin 1A-GFP | Sci Signal. 2016 |
| Ezrin | Ezrin-GFP | PLoS One 2015 |
| Grb2 | Grb2-GFP | PLoS One 2015 |
| HS1 | HS1-GFP | Sci Signal. 2016 |
| Itk | Itk-GFP | PLoS One 2015 |
| LAT | LAT-GFP | Sci Signal. 2009 |
| Lck | Lck-GFP | PLoS One 2015 |
| Myosin II RLC | Myosin II RLC-GFP | Sci Signal. 2016 |
| NF$\kappa$B p65 | GFP-p65 | PLoS One 2015 |
| $PIP_2$ | GFP-PLC$\delta$-PH | PLoS One 2015 |
| PKC $\Theta$ | PKC $\Theta$-GFP | Sci Signal. 2009 |
| Rac | POSH GBD-GFP-CAAX | Sci Signal. 2009 |
| SLP-76 | SLP-76-GFP | PLoS One 2015 |
| TCR as TCR$\zeta$ | TCR$\zeta$-GFP | Sci Signal. 2009 |
| Vav1 | Vav1-GFP | PLoS One 2015 |
| WASP | GFP-WASP | Sci Signal. 2016 |
| WAVE-2 | GFP-WAVE2 | Sci Signal. 2016 |

| Condition | Comparison | Pattern | -40 | -20 | 0 | 20 | 40 | 60 | 80 | 100 | 120 | 180 | 300 | 420 |
|---|---|---|---|---|---|---|---|---|---|---|---|---|---|---|
| LAT, anti-B7 | LAT, full stim. | any | | | 0.000 | 0.000 | 0.000 | 0.000 | 0.000 | 0.000 | 0.000 | 0.005 | 0.04 | 0.02 |
| | | central | | | 0.000 | 0.000 | 0.001 | 0.006 | | | | | | |
| LAT, Itk ko, full stim. | LAT, full stim. | any | | | 0.000 | | | | | | | | | |
| | | central | | | 0.005 | 0.02 | | | | | | | | |
| LAT, Itk ko, anti-B7 | LAT, full stim. | any | | | 0.000 | 0.000 | 0.000 | 0.000 | 0.000 | 0.000 | 0.000 | 0.000 | 0.02 | 0.005 |
| | | central | | | 0.000 | 0.000 | 0.05 | 0.01 | 0.03 | 0.05 | | 0.03 | | |
| LAT, Itk ko, anti-B7, Rac Cofilin | LAT, full stim. | any | | | 0.001 | 0.001 | | | | | | 0.02 | 0.007 | 0.008 |
| | | central | | | 0.008 | | | | 0.02 | 0.000 | 0.000 | 0.01 | 0.05 | |
| LAT, Itk ko, anti-B7, Rac Cofilin | LAT, Itk ko, anti-B7 | any | | | | | 0.006 | 0.000 | 0.000 | 0.000 | 0.000 | 0.000 | 0.000 | 0.000 |
| | | central | | | | 0.03 | 0.01 | 0.002 | 0.000 | 0.000 | 0.000 | 0.000 | 0.02 | |

## Table S2

## LAT V3

| Condition | Comparison | Pattern | -40 | -20 | 0 | 20 | 40 | 60 | 80 | 100 | 120 | 180 | 300 | 420 |
|---|---|---|---|---|---|---|---|---|---|---|---|---|---|---|
| **Restoration to LAT full stimulus** | | | | | | | | | | | | | | |
| LAT V3, full stimulus | LAT, full stimulus | any | | | 0.03 | 0.001 | 0.000 | 0.000 | 0.000 | 0.000 | 0.000 | 0.000 | 0.000 | 0.000 |
| | | central | | | | | 0.004 | 0.001 | 0.000 | 0.000 | 0.000 | 0.000 | 0.03 | 0.002 |
| LAT V3, Itk ko, full stimulus | LAT, full stimulus | any | | 0.002 | | | 0.04 | 0.01 | 0.004 | 0.003 | 0.002 | 0.001 | 0.001 | 0.000 |
| | | central | | | 0.01 | | 0.007 | 0.006 | 0.000 | 0.000 | 0.000 | 0.000 | 0.004 | 0.006 |
| LAT V3, anti-B7 | LAT, full stimulus | any | | 0.006 | | 0.008 | 0.002 | 0.004 | 0.003 | 0.000 | 0.000 | 0.000 | 0.006 | 0.006 |
| | | central | | | | | 0.04 | 0.03 | 0.02 | 0.000 | 0.000 | 0.000 | | |
| LAT V3, Itk ko anti-B7 | LAT, full stimulus | any | | | 0.000 | 0.006 | | | | | | 0.01 | 0.009 | 0.02 |
| | | central | | | 0.000 | | 0.000 | 0.000 | 0.000 | 0.000 | 0.000 | 0.000 | 0.03 | 0.003 |
| **Enhancement under matched stimuli** | | | | | | | | | | | | | | |
| LAT V3, Itk ko, full stimulus | LAT, Itk ko, full stimulus | any | | 0.004 | 0.007 | | | | 0.03 | 0.01 | 0.004 | 0.04 | 0.01 | 0.001 |
| | | central | | | | 0.03 | 0.01 | 0.005 | 0.001 | 0.000 | 0.001 | 0.001 | 0.006 | 0.004 |
| LAT V3, anti-B7 | LAT, anti-B7 | any | | | | | 0.002 | 0.001 | 0.000 | 0.000 | 0.000 | 0.000 | 0.006 | 0.003 |
| | | central | | | | 0.02 | 0.000 | 0.000 | 0.000 | 0.000 | 0.000 | 0.000 | 0.003 | 0.004 |
| LAT V3, Itk ko, anti-B7 | LAT, Itk ko, anti-B7 | any | | 0.000 | 0.000 | 0.000 | 0.000 | 0.000 | 0.000 | 0.000 | 0.000 | 0.000 | 0.001 | 0.000 |
| | | central | | | 0.04 | 0.001 | 0.000 | 0.000 | 0.000 | 0.000 | 0.000 | 0.000 | 0.01 | 0.000 |

## LAT Vav

| Condition | Comparison | Pattern | -40 | -20 | 0 | 20 | 40 | 60 | 80 | 100 | 120 | 180 | 300 | 420 |
|---|---|---|---|---|---|---|---|---|---|---|---|---|---|---|
| **Restoration to LAT full stimulus** | | | | | | | | | | | | | | |
| LAT Vav, full stimulus | LAT, full stimulus | any | | | 0.002 | 0.03 | 0.004 | 0.002 | 0.001 | 0.003 | 0.000 | 0.002 | | |
| | | central | | | 0.05 | 0.01 | | | | | | | | |
| LAT Vav, Itk ko, full stimulus | LAT, full stimulus | any | | | 0.000 | 0.001 | | | | | | | 0.008 | |
| | | central | | | 0.005 | | | 0.001 | 0.001 | 0.000 | 0.000 | 0.001 | | |
| LAT Vav, anti-B7 | LAT, full stimulus | any | | | | | | | | | | | | |
| | | central | | | | | 0.002 | 0.002 | 0.002 | 0.000 | 0.002 | | | |
| LAT Vav, Itk ko anti-B7 | LAT, full stimulus | any | | | 0.000 | 0.000 | | | | | | 0.04 | | |
| | | central | | | 0.000 | | 0.02 | 0.006 | 0.000 | 0.000 | 0.000 | 0.002 | | 0.05 |
| **Enhancement under matched stimuli** | | | | | | | | | | | | | | |
| LAT Vav, Itk ko, full stimulus | LAT, Itk ko, full stimulus | any | | | | 0.01 | 0.05 | | | | | | 0.05 | |
| | | central | | | | | | 0.001 | 0.05 | 0.02 | 0.03 | 0.005 | | |
| LAT Vav, anti-B7 | LAT, anti-B7 | any | | | 0.001 | 0.01 | 0.000 | 0.000 | 0.001 | 0.001 | 0.005 | | | 0.03 |
| | | central | | | 0.000 | 0.000 | 0.000 | 0.000 | 0.001 | 0.000 | 0.000 | | | |
| LAT Vav, Itk ko, anti-B7 | LAT, Itk ko, anti-B7 | any | | | | 0.03 | 0.001 | 0.000 | 0.000 | 0.000 | 0.000 | 0.000 | 0.001 | 0.000 |
| | | central | | | | 0.005 | 0.000 | 0.000 | 0.000 | 0.000 | 0.000 | 0.000 | 0.03 | 0.007 |

## LAT PLCdPH

| Condition | Comparison | Pattern | -40 | -20 | 0 | 20 | 40 | 60 | 80 | 100 | 120 | 180 | 300 | 420 |
|---|---|---|---|---|---|---|---|---|---|---|---|---|---|---|
| **Restoration to LAT full stimulus** | | | | | | | | | | | | | | |
| LAT PLCd, full stimulus | LAT, full stimulus | any | | | 0.000 | 0.000 | 0.000 | 0.002 | 0.03 | 0.03 | | | | |
| | | central | | | 0.000 | 0.05 | | | | | | | | |
| LAT PLCd, Itk ko, full stimulus | LAT, full stimulus | any | | | 0.000 | 0.01 | | | 0.001 | | 0.03 | | | |
| | | central | | | 0.001 | | | | 0.05 | 0.04 | | | | |
| LAT PLCd, anti-B7 | LAT, full stimulus | any | | | | 0.03 | 0.01 | 0.002 | 0.000 | 0.000 | 0.000 | 0.000 | 0.001 | 0.05 |
| | | central | | | | 0.009 | | | | | | | | 0.04 |
| LAT PLCd, Itk ko anti-B7 | LAT, full stimulus | any | | | 0.000 | 0.009 | | | | | | 0.005 | | |
| | | central | | | 0.001 | 0.02 | | | | | | | | |
| **Enhancement under matched stimuli** | | | | | | | | | | | | | | |
| LAT PLCd, Itk ko, full stimulus | LAT, Itk ko, full stimulus | any | | | | | | | 0.005 | | 0.05 | | | |
| | | central | 0.05 | | | | | | | | | | | |
| LAT PLCd, anti-B7 | LAT, anti-B7 | any | | | 0.009 | | | 0.03 | | | | | | |
| | | central | | | 0.01 | | | | | | | | | |
| LAT PLCd, Itk ko anti-B7 | LAT, Itk ko, anti-B7 | any | | | | 0.005 | 0.002 | 0.000 | 0.000 | 0.000 | 0.000 | 0.000 | 0.002 | 0.002 |
| | | central | | | | | | | | 0.003 | 0.05 | | | |

**Table S3**

| Condition | Comparison | Pattern | -40 | -20 | 0 | 20 | 40 | 60 | 80 | 100 | 120 | 180 | 300 | 420 |
|---|---|---|---|---|---|---|---|---|---|---|---|---|---|---|
| Grb2 + LATV3, full stimulus | Grb2, full stimulus | any<br>central | | | 0.01 | 0.000 | 0.003 | 0.001 | 0.000 | 0.02<br>(0.07) | (0.06) | 0.003 | | |
| Grb2 + LATV3, Itk ko, full stim. | Grb2, Itk ko, full stim | any<br>central | (0.06) | 0.03 | | | 0.04 | (0.07) | 0.02<br>0.001 | 0.03<br>0.001 | 0.01 | | 0.009 | |
| Grb2 + LATV3, anti-B7 | Grb2, anti-B7 | any<br>central | 0.05 | 0.002<br>0.05 | 0.000 | 0.02 | 0.02 | | 0.009 | | (0.06) | (0.06)<br>0.04 | 0.04 | (0.06) |
| Lck + LATV3, full stimulus | Lck, full stimulus | any<br>central | | 0.04<br>0.03 | | 0.02<br>0.000 | 0.04<br>0.001 | 0.001<br>0.000 | 0.001<br>0.008 | 0.001<br>0.008 | 0.000<br>0.05 | 0.000<br>(0.06) | 0.000<br>0.007 | 0.001 |
| Lck + LATV3, Itk ko, full stim. | Lck, Itk ko, full stim | any<br>central | | | | 0.02 | 0.000<br>0.007 | 0.001<br>0.003 | 0.04<br>(0.07) | 0.02 | | | | 0.02 |
| Lck + LATV3, anti-B7 | Lck, anti-B7 | any<br>central | 0.05<br>0.05 | (0.06) | | 0.03 | | | | | | | | |
| Vav1 + LATV3, full stimulus | Vav1, full stimulus | any<br>central | | 0.000<br>0.002 | 0.000<br>0.002 | 0.000<br>0.02 | 0.006 | 0.009 | 0.03 | 0.001 | | 0.02 | | |
| Vav1 + LATV3, Itk ko, full stim. | Vav1, Itk ko, full stim | any<br>central | (0.06) | | | (0.06) | | | | | | | | |
| Vav1 + LATV3, anti-B7 | Vav1, anti-B7 | any<br>central | | 0.000<br>0.01 | 0.02 | 0.02 | 0.05 | 0.03 | 0.03 | | | | (0.06) | |

## Table S4

| Condition | Comparison | Pattern | -40 | -20 | 0 | 20 | 40 | 60 | 80 | 100 | 120 | 180 | 300 | 420 |
|---|---|---|---|---|---|---|---|---|---|---|---|---|---|---|
| SLP-76, anti-B7 | SLP-76, full stimulus | any | | | | 0.005 | 0.000 | 0.000 | 0.000 | 0.000 | 0.001 | 0.002 | | |
| | | central | | | 0.01 | 0.005 | 0.02 | 0.005 | | | | | | 0.01 |
| SLP-76, ltk ko, full stim. | SLP-76, full stimulus | any | | 0.05 | | 0.001 | 0.000 | 0.003 | 0.000 | 0.000 | 0.000 | 0.006 | | |
| | | central | | | 0.000 | 0.002 | 0.002 | 0.003 | 0.04 | 0.04 | 0.05 | | | |
| SLP-76, ltk ko, anti-B7 | SLP-76, full stimulus | any | | | 0.03 | 0.003 | 0.001 | 0.001 | 0.008 | 0.003 | | | | |
| | | central | | | 0.000 | 0.006 | | | | 0.04 | | | | |

## Table S5

## SLP-76 V3

| Condition | Comparison | Pattern | -40 | -20 | 0 | 20 | 40 | 60 | 80 | 100 | 120 | 180 | 300 | 420 |
|---|---|---|---|---|---|---|---|---|---|---|---|---|---|---|
| **Restoration to SLP-76 full stimulus** | | | | | | | | | | | | | | |
| SLP-76 V3, full stimulus | SLP-76, full stimulus | any central | | 0.04 | | 0.03 | | | | | | | | |
| SLP-76 V3, Itk ko, full stimulus | SLP-76, full stimulus | any central | 0.01 | 0.000<br>0.03 | 0.01<br>0.03 | 0.04 | 0.02 | | | | 0.05 | | 0.03 | 0.003 |
| SLP-76 V3, anti-B7 | SLP-76, full stimulus | any central | | | | | | | 0.000 | 0.000<br>0.05 | 0.000 | 0.005 | | |
| SLP-76 V3, Itk ko anti-B7 | SLP-76, full stimulus | any central | | | 0.02 | | 0.03<br>0.04 | 0.05 | 0.000 | 0.001 | | 0.02 | | |
| **Enhancement under matched stimuli** | | | | | | | | | | | | | | |
| SLP-76 V3, Itk ko, full stimulus | SLP-76, Itk ko, full stimulus | any central | | 0.000 | 0.000 | 0.000 | 0.000<br>0.05 | 0.000 | 0.000 | 0.000 | 0.000 | 0.000 | 0.001 | 0.000 |
| SLP-76 V3, anti-B7 | SLP-76, anti-B7 | any central | | | 0.008<br>0.002 | 0.008 | 0.005<br>0.03 | | | | 0.02 | | | |
| SLP-76 V3, Itk ko anti-B7 | SLP-76, Itk ko, anti-B7 | any central | 0.05 | | | 0.03 | 0.004 | | | | | | | |

## SLP-76 Vav

| Condition | Comparison | Pattern | -40 | -20 | 0 | 20 | 40 | 60 | 80 | 100 | 120 | 180 | 300 | 420 |
|---|---|---|---|---|---|---|---|---|---|---|---|---|---|---|
| **Restoration to SLP-76 full stimulus** | | | | | | | | | | | | | | |
| SLP-76 Vav, full stimulus | SLP-76, full stimulus | any central | | | | | | | | | | | | |
| SLP-76 Vav, Itk ko, full stimulus | SLP-76, full stimulus | any central | | 0.03<br>0.02 | | | 0.04 | 0.03 | 0.01<br>0.006 | 0.02<br>0.05 | | | | |
| SLP-76 Vav, anti-B7 | SLP-76, full stimulus | any central | | | 0.01<br>0.04 | 0.006 | 0.04 | 0.003 | 0.000 | 0.000 | 0.001 | 0.000 | | 0.03 |
| SLP-76 Vav, Itk ko anti-B7 | SLP-76, full stimulus | any central | | 0.03<br>0.02 | | | 0.04 | 0.03 | 0.01<br>0.006 | 0.02<br>0.05 | | | | |
| **Enhancement under matched stimuli** | | | | | | | | | | | | | | |
| SLP-76 Vav, Itk ko, full stimulus | SLP-76, Itk ko, full stimulus | any central | | | 0.003 | | 0.02<br>0.007 | 0.03 | 0.006 | 0.004 | 0.04 | | 0.02 | |
| SLP-76 Vav, anti-B7 | SLP-76, anti-B7 | any central | | | 0.000<br>0.000 | 0.001<br>0.000 | 0.02 | 0.01 | | | | | | |
| SLP-76 Vav, Itk ko anti-B7 | SLP-76, Itk ko, anti-B7 | any central | 0.05 | | 0.007<br>0.02 | 0.02<br>0.02 | 0.03 | 0.01 | | | 0.05 | | | |

**Table S6**

| Condition | Comparison | Pattern | -40 | -20 | 0 | 20 | 40 | 60 | 80 | 100 | 120 | 180 | 300 | 420 |
|---|---|---|---|---|---|---|---|---|---|---|---|---|---|---|
| Grb2, anti-B7 | Grb2, full stimulus | any<br>central | | | | 0.001<br>0.04 | | 0.02<br>0.05 | 0.02 | | | | | |
| Grb2, Itk ko, full stim. | Grb2, full stimulus | any<br>central | 0.03 | | 0.001 | 0.000 | 0.000 | 0.000 | 0.000 | 0.008 | | 0.01 | | |
| Grb2, Itk ko, anti-B7 | Grb2, full stimulus | any<br>central | | | 0.002<br>0.02 | 0.000<br>0.003 | 0.000<br>0.05 | 0.002<br>0.006 | 0.006 | 0.03 | | | | |

## Table S7

## Grb2 V3

| Condition | Comparison | Pattern | -40 | -20 | 0 | 20 | 40 | 60 | 80 | 100 | 120 | 180 | 300 | 420 |
|---|---|---|---|---|---|---|---|---|---|---|---|---|---|---|
| **Restoration to Grb2 full stimulus** | | | | | | | | | | | | | | |
| Grb2 V3, full stimulus | Grb2, full stimulus | any | | | | | | | | | | | | 0.02 |
| | | central | | | | 0.000 | | | | | | | | 0.05 |
| Grb2 V3, Itk ko, full stimulus | Grb2, full stimulus | any | | 0.02 | | 0.000 | 0.004 | 0.004 | 0.002 | | | | | 0.02 |
| | | central | | | | | | 0.006 | | | | | | |
| Grb2 V3, anti-B7 | Grb2, full stimulus | any | | | | | | | | | | | | 0.04 |
| | | central | | | | 0.001 | | | | 0.04 | | | | |
| Grb2 V3, Itk ko anti-B7 | Grb2, full stimulus | any | | | 0.000 | 0.000 | 0.000 | 0.000 | 0.000 | 0.001 | | | | |
| | | central | | | 0.01 | 0.01 | | 0.04 | | | | | | |
| **Enhancement under matched stimuli** | | | | | | | | | | | | | | |
| Grb2 V3, Itk ko, full stimulus | Grb2, Itk ko, full stimulus | any | | 0.01 | | | | | | | | | 0.03 | |
| | | central | | | | | | 0.03 | | | | | 0.05 | |
| Grb2 V3, anti-B7 | Grb2, anti-B7 | any | | | | | | | | | | | | |
| | | central | 0.05 | 0.05 | | | | | | 0.04 | | | | |
| Grb2 V3, Itk ko anti-B7 | Grb2, Itk ko, anti-B7 | any | 0.04 | 0.02 | 0.04 | | | 0.02 | 0.02 | | | | | |
| | | central | | | | | | | 0.04 | | | | | |

## Grb2 Vav

| Condition | Comparison | Pattern | -40 | -20 | 0 | 20 | 40 | 60 | 80 | 100 | 120 | 180 | 300 | 420 |
|---|---|---|---|---|---|---|---|---|---|---|---|---|---|---|
| **Restoration to Grb2 full stimulus** | | | | | | | | | | | | | | |
| Grb2 Vav, full stimulus | Grb2, full stimulus | any | 0.05 | 0.000 | 0.000 | | 0.05 | | | 0.05 | 0.002 | 0.000 | 0.02 | 0.04 |
| | | central | | | 0.01 | 0.03 | | 0.04 | | | | | 0.05 | |
| | | periphery | | 0.000 | 0.000 | 0.000 | 0.000 | 0.000 | 0.000 | 0.000 | 0.000 | 0.000 | 0.000 | 0.005 |
| Grb2 Vav, Itk ko, full stimulus | Grb2, full stimulus | any | 0.03 | 0.000 | 0.001 | | 0.02 | 0.04 | 0.01 | 0.000 | 0.000 | 0.000 | 0.002 | |
| | | central | | | 0.02 | 0.001 | 0.03 | 0.01 | 0.03 | 0.04 | | | 0.05 | |
| | | periphery | | 0.000 | 0.000 | 0.000 | 0.000 | 0.000 | 0.000 | 0.000 | 0.000 | 0.000 | 0.007 | 0.04 |
| Grb2 Vav, anti-B7 | Grb2, full stimulus | any | 0.04 | 0.000 | 0.000 | | | | | | | | | |
| | | central | | | 0.01 | | | 0.05 | | | | | | |
| | | periphery | | 0.001 | 0.000 | 0.000 | 0.000 | 0.000 | 0.000 | 0.02 | 0.01 | | | |
| Grb2 Vav, Itk ko anti-B7 | Grb2, full stimulus | any | | 0.000 | 0.01 | | 0.05 | | 0.03 | 0.01 | 0.001 | 0.007 | | 0.04 |
| | | central | | 0.03 | 0.000 | 0.01 | 0.003 | | 0.02 | 0.04 | | 0.03 | 0.05 | 0.03 |
| | | periphery | | 0.002 | 0.000 | 0.000 | 0.000 | 0.000 | 0.000 | 0.000 | 0.000 | 0.000 | 0.04 | 0.03 |
| **Enhancement under matched stimuli** | | | | | | | | | | | | | | |
| Grb2 Vav, Itk ko, full stimulus | Grb2, Itk ko, full stimulus | any | | 0.000 | 0.000 | 0.000 | 0.000 | 0.000 | 0.000 | 0.000 | 0.000 | 0.000 | 0.000 | |
| | | central | | | | 0.02 | 0.02 | 0.05 | | 0.05 | 0.04 | 0.03 | 0.05 | 0.05 |
| | | periphery | | 0.000 | 0.000 | 0.000 | 0.000 | 0.000 | 0.000 | 0.000 | 0.000 | 0.000 | 0.003 | |
| Grb2 Vav, anti-B7 | Grb2, anti-B7 | any | | 0.002 | 0.000 | 0.000 | | | | | | | | |
| | | central | 0.05 | | | | | | | | | | | 0.05 |
| | | periphery | | 0.007 | 0.000 | 0.000 | 0.004 | 0.000 | 0.001 | 0.004 | 0.008 | | | |
| Grb2 Vav, Itk ko anti-B7 | Grb2, Itk ko, anti-B7 | any | | 0.03 | 0.000 | 0.000 | 0.000 | 0.000 | 0.000 | 0.000 | 0.004 | 0.01 | | |
| | | central | | 0.02 | 0.01 | 0.02 | 0.02 | 0.02 | 0.01 | 0.03 | 0.02 | 0.01 | 0.02 | 0.01 |
| | | periphery | | | 0.001 | 0.000 | 0.000 | 0.000 | 0.000 | 0.000 | 0.000 | 0.009 | | 0.04 |

**Table S8**

**Figure 1**

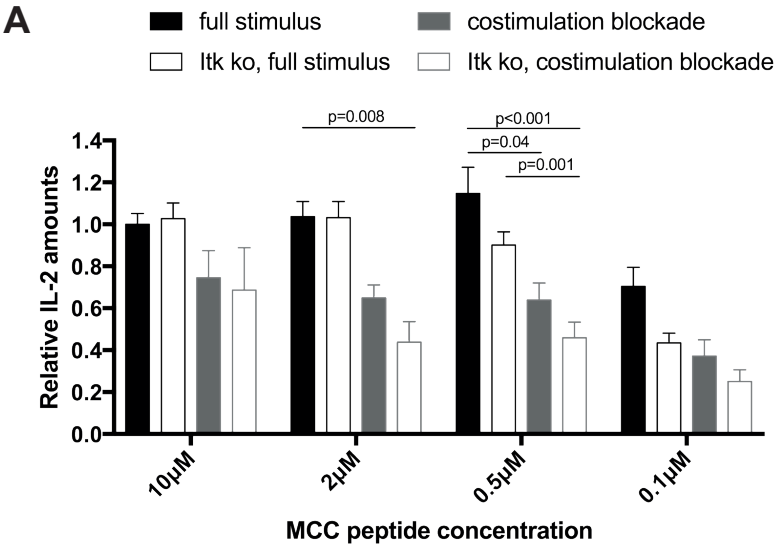
A
full stimulus
costimulation blockade
Itk ko, full stimulus
Itk ko, costimulation blockade
p=0.008
p<0.001
p=0.04
p=0.001
Relative IL-2 amounts
1.4
1.2
1.0
0.8
0.6
0.4
0.2
0.0
10μM
2μM
0.5μM
0.1μM
MCC peptide concentration

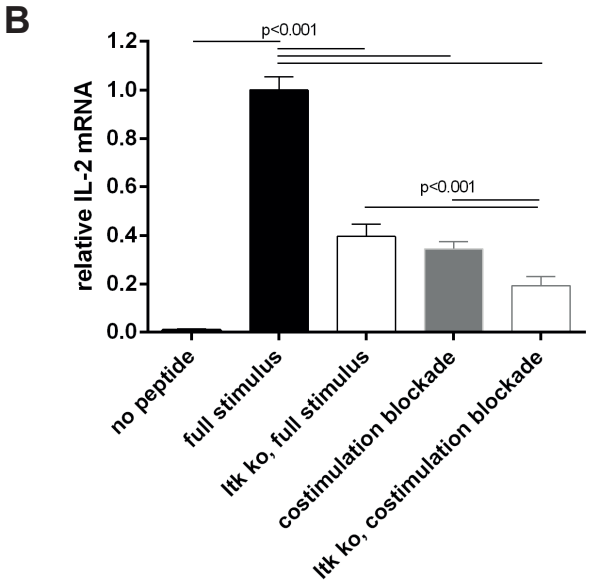
B
p<0.001
p<0.001
relative IL-2 mRNA
1.2
1.0
0.8
0.6
0.4
0.2
0.0
no peptide
full stimulus
Itk ko, full stimulus
costimulation blockade
Itk ko, costimulation blockade

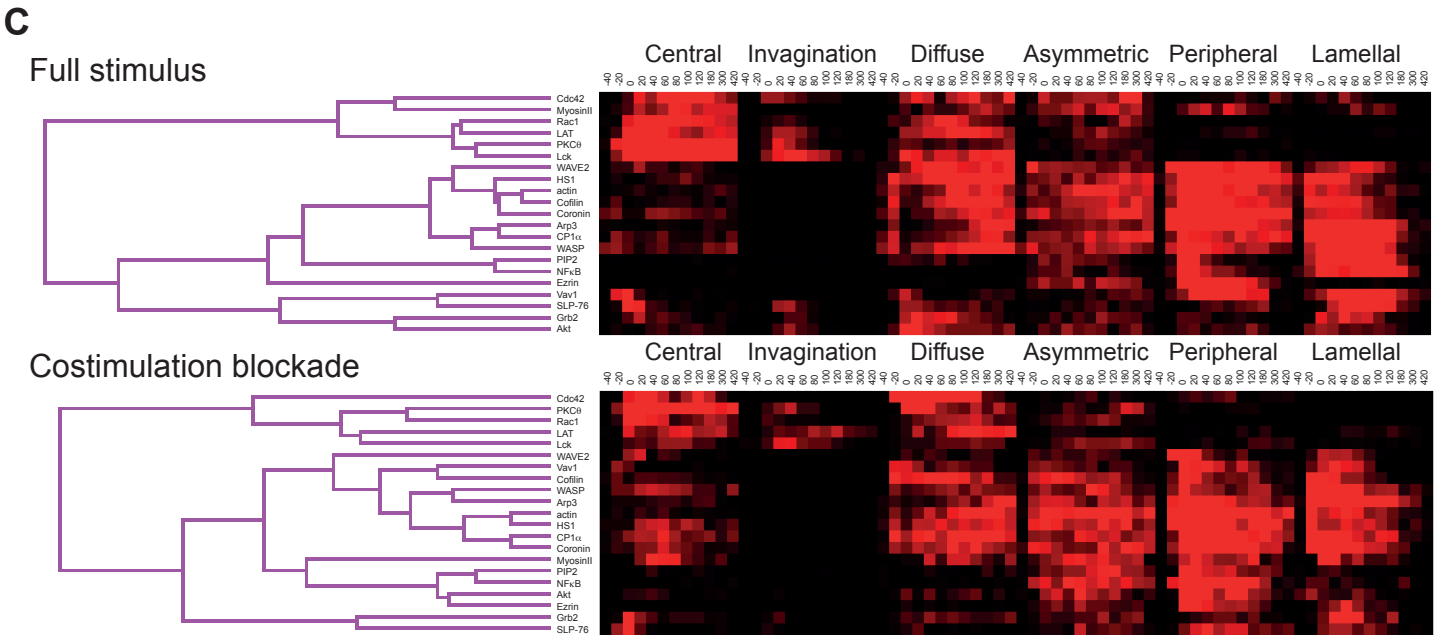
C
Full stimulus
Central
Invagination
Diffuse
Asymmetric
Peripheral
Lamellal
Cdc42
MyosinII
Rac1
LAT
PKCθ
Lck
WAVE2
HS1
actin
Cofilin
Coronin
Arp3
CP1α
WASP
PIP2
NFκB
Ezrin
Vav1
SLP-76
Grb2
Akt
Costimulation blockade
Central
Invagination
Diffuse
Asymmetric
Peripheral
Lamellal
Cdc42
PKCθ
Rac1
LAT
Lck
WAVE2
Vav1
Cofilin
WASP
Arp3
actin
HS1
CP1α
Coronin
MyosinII
PIP2
NFκB
Akt
Ezrin
Grb2
SLP-76

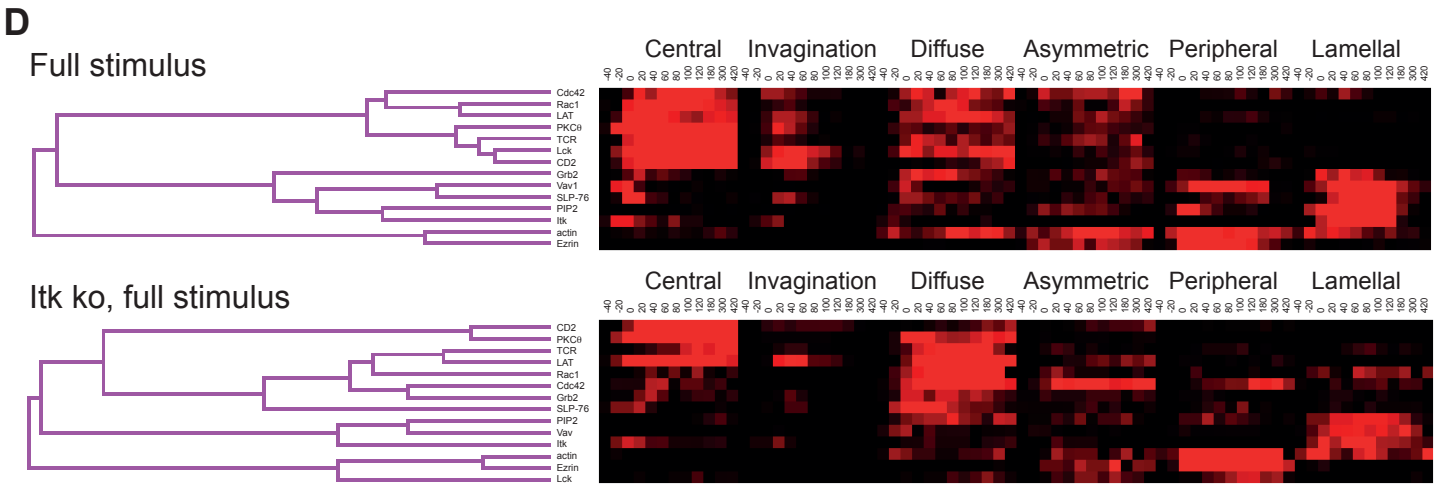
D
Full stimulus
Central
Invagination
Diffuse
Asymmetric
Peripheral
Lamellal
Cdc42
Rac1
LAT
PKCθ
TCR
Lck
CD2
Grb2
Vav1
SLP-76
PIP2
Itk
actin
Ezrin
Itk ko, full stimulus
Central
Invagination
Diffuse
Asymmetric
Peripheral
Lamellal
CD2
PKCθ
TCR
LAT
Rac1
Cdc42
Grb2
SLP-76
PIP2
Vav
Itk
actin
Ezrin
Lck

# Figure 2

**A**

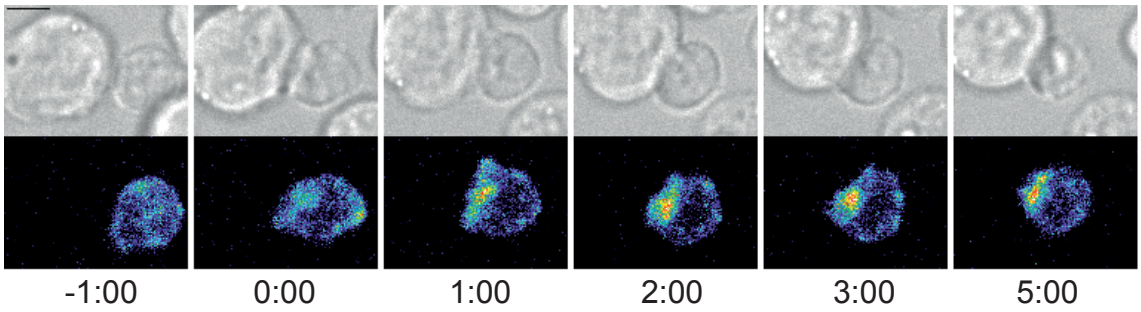


**B**

Full stimulus

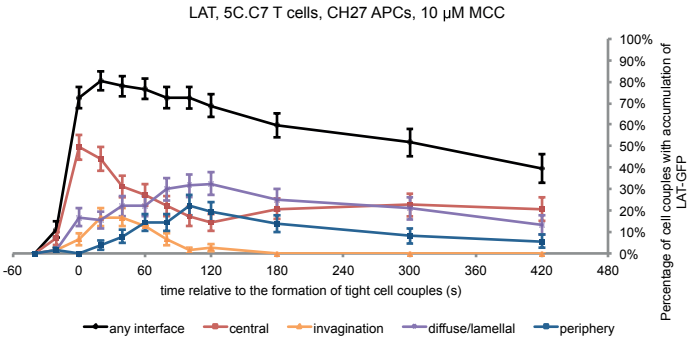


Itk ko, full stimulus

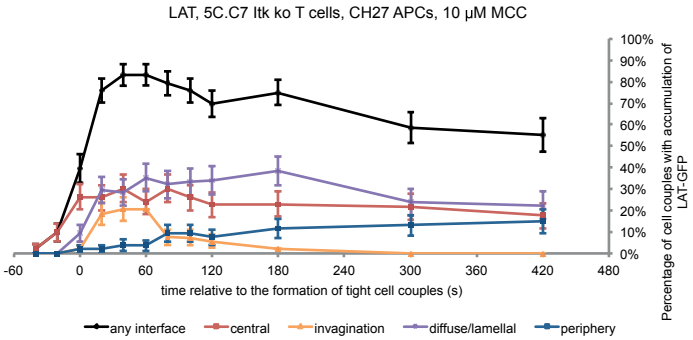


Costimulation blockade

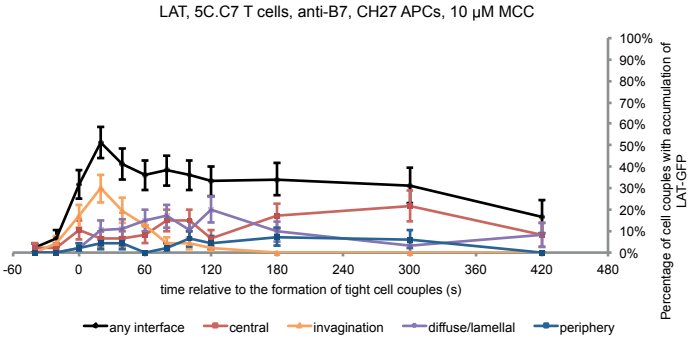


Itk ko, costimulation blockade

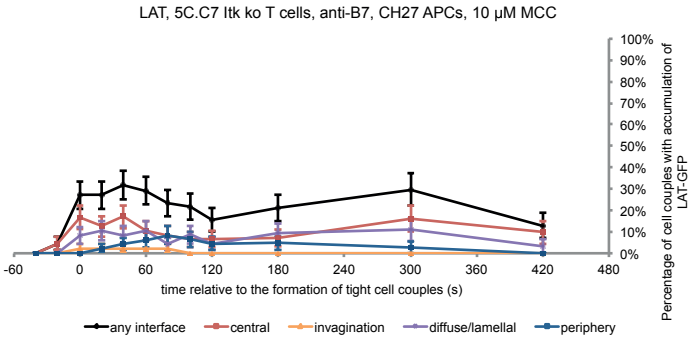


**C**

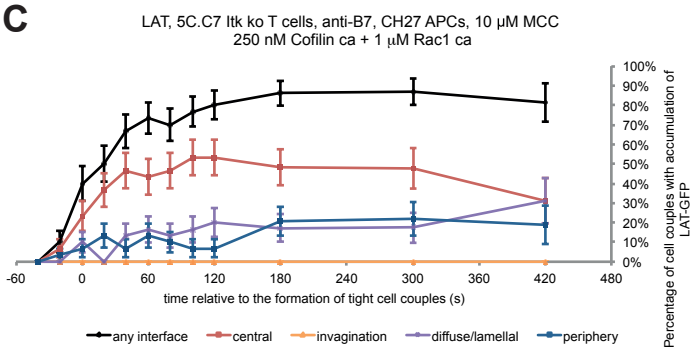


**D**

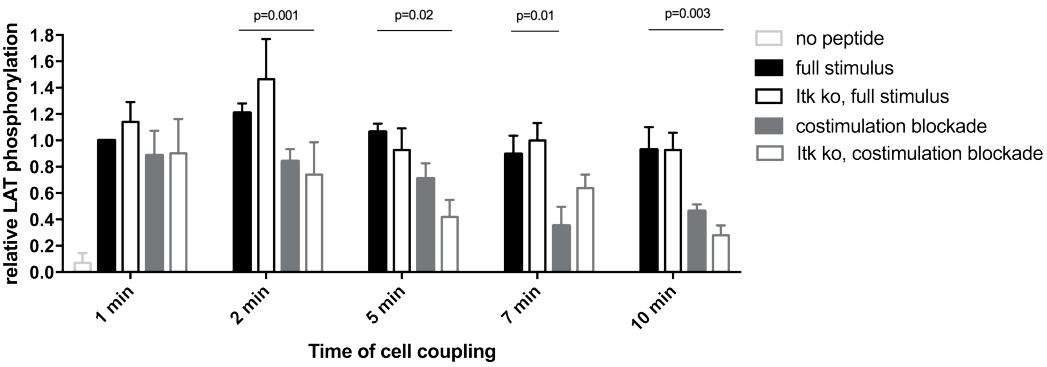

# Figure 3

**A**

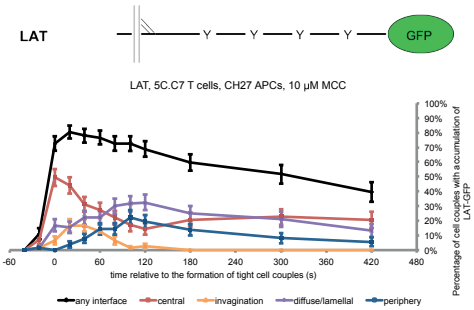


**B**

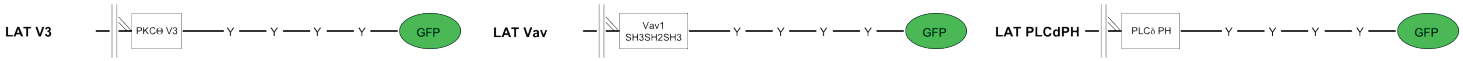


## Full stimulus

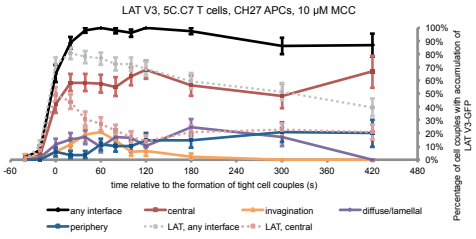


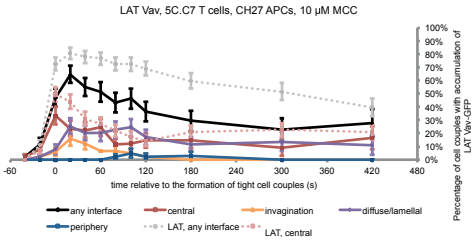


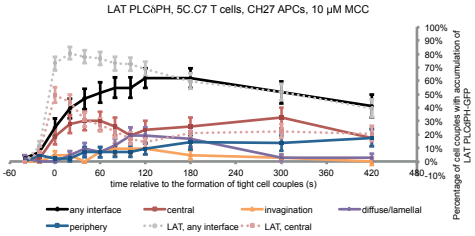


## Itk ko, full stimulus

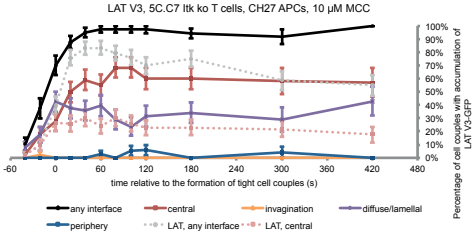


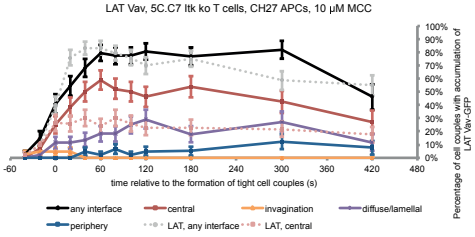


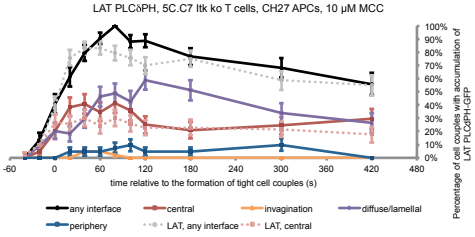


## Costimulation blockade

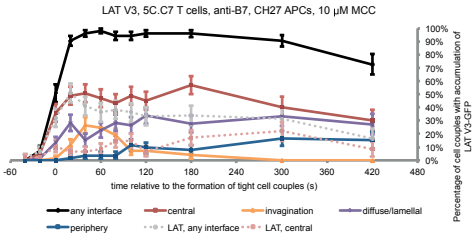


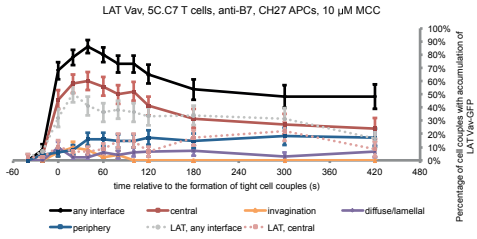


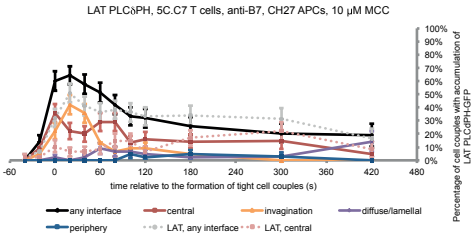


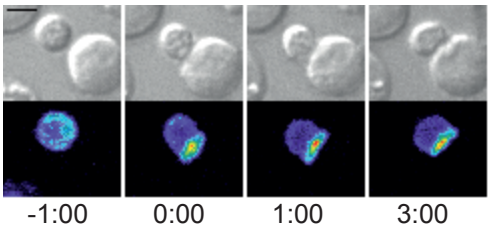


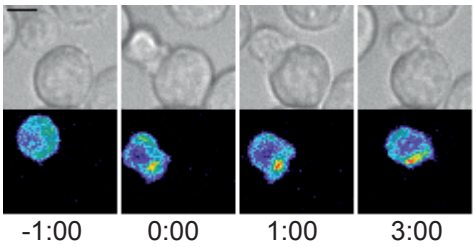


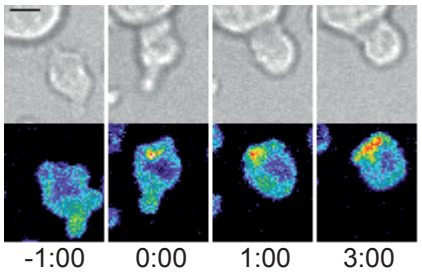


## Itk ko, costimulation blockade

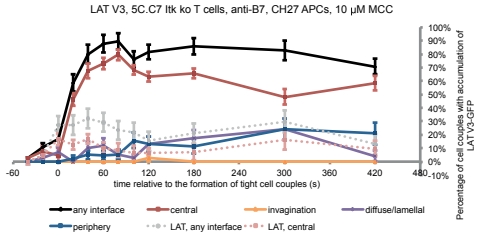


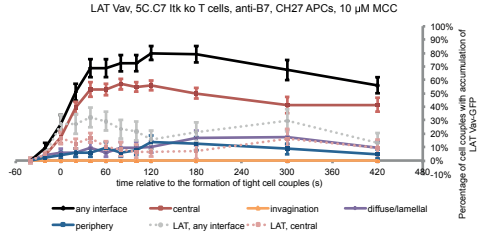


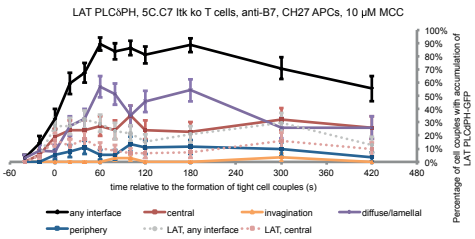

# Figure 4

**A**

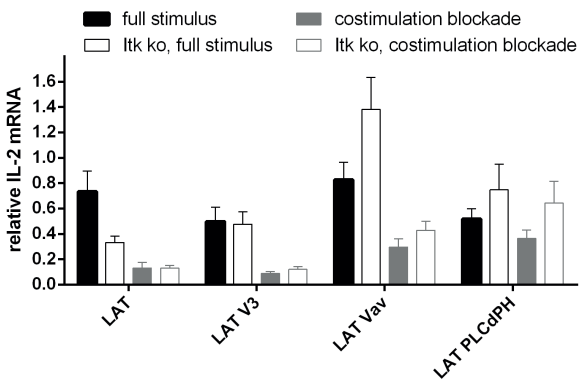


Statistical significance of differences in relative IL-2 mRNA

| | Comparison | LAT | LAT V3 | LAT Vav | LAT PLCdPH |
|---|---|---|---|---|---|
| LAT, full stimulus | anti-B7 | 0.000 | 0.000 | | |
| | Itk ko, anti-B7 | 0.001 | 0.004 | | |
| LAT, Itk ko, full stim. | Itk ko, full stim. | | | 0.001 | |
| LAT, anti-B7 | anti-B7 | | | 0.007 | 0.002 |
| LAT, Itk ko, anti-B7 | Itk ko, anti-B7 | | | 0.03 | |

**B** Relations between enhanced/diminished central adaptor localization and full/reduced IL-2 mRNA amounts

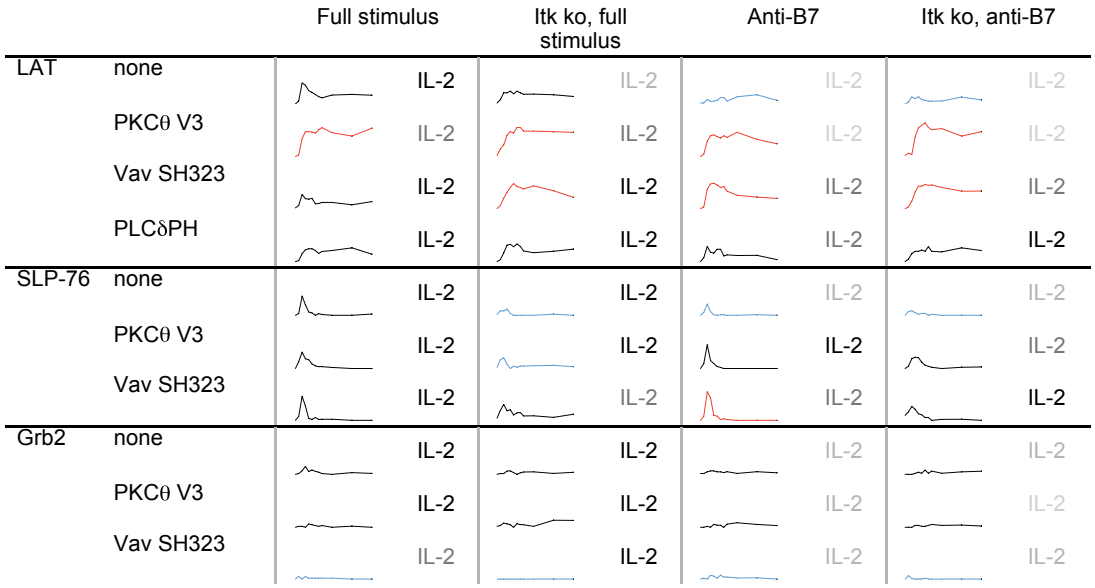


**C** LAT V3 + Grb2-GFP LAT V3 + Lck-GFP LAT V3 + Vav-1 GFP

Full stimulus

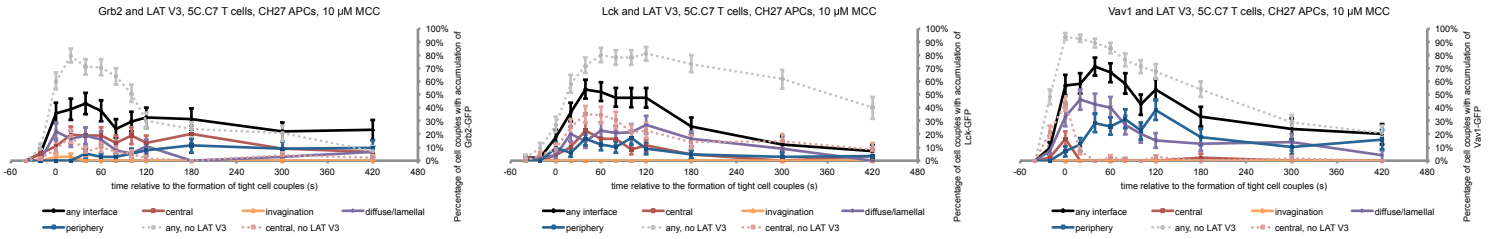


Itk ko, full stimulus

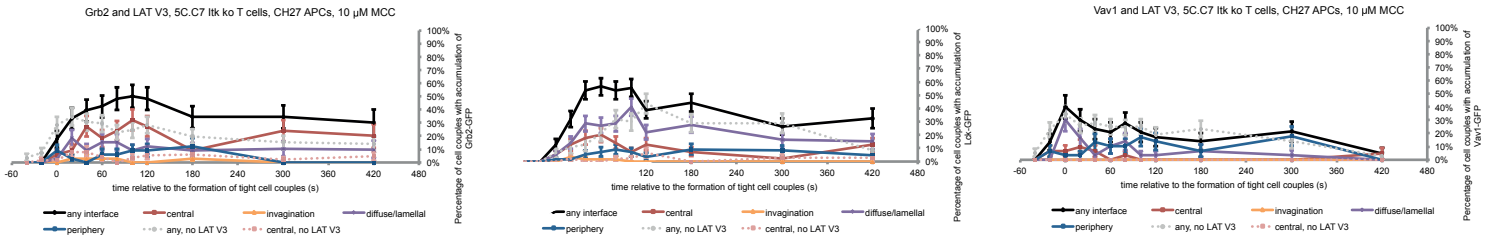


Costimulation blockade

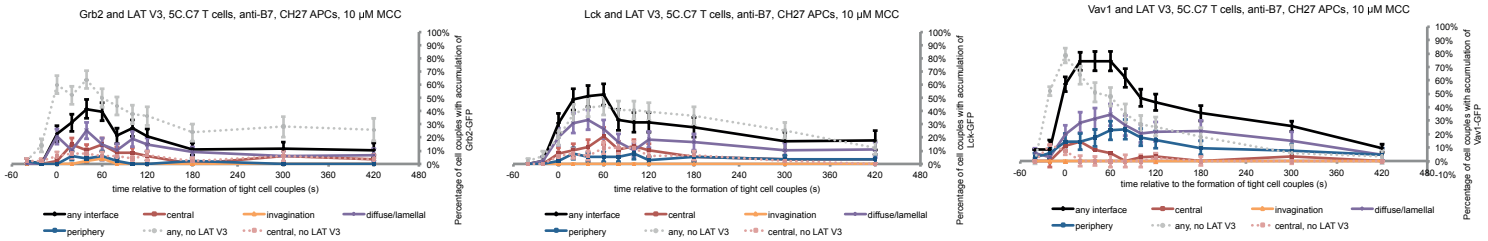

**Figure 5**

**A**

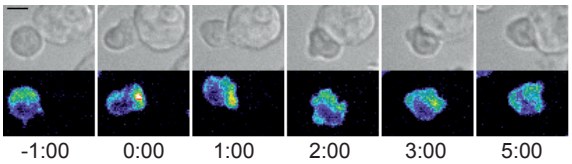


**B**

Full stimulus

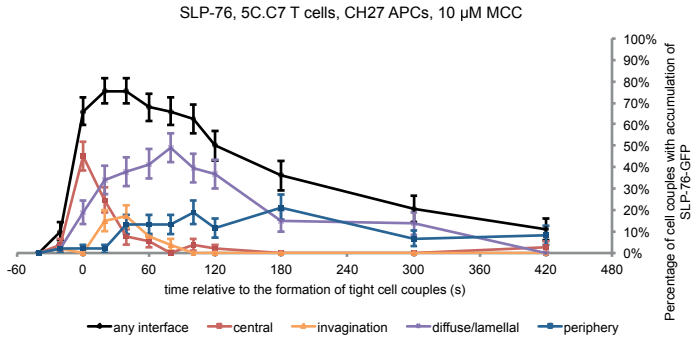


Itk ko, full stimulus

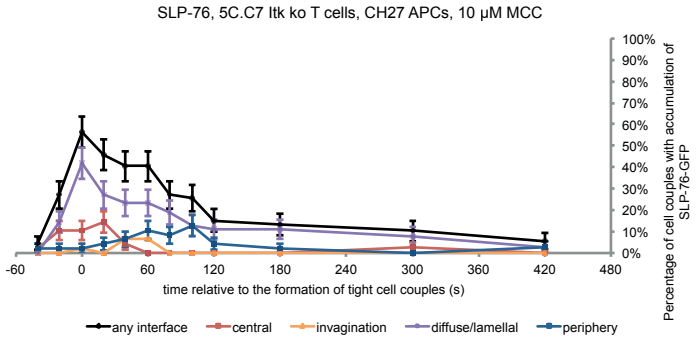


Costimulation blockade

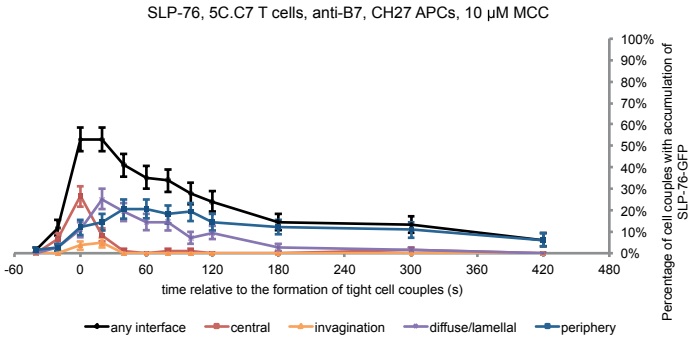


Itk ko, costimulation blockade

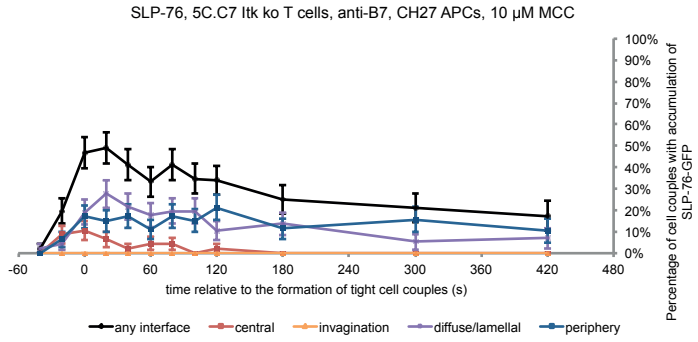

# Figure 6

## A

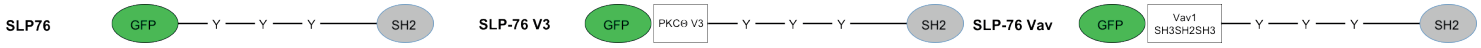


### Full stimulus

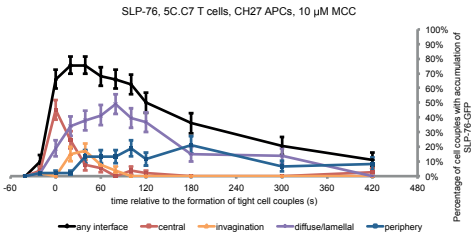


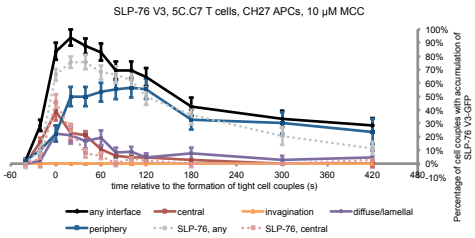


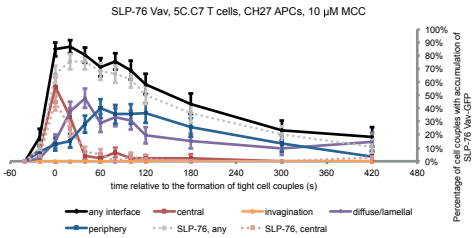


### Itk ko, full stimulus

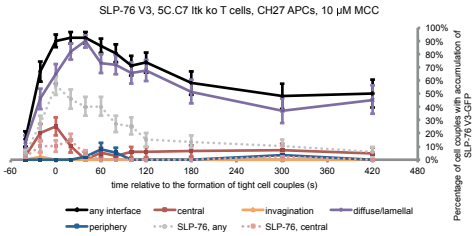


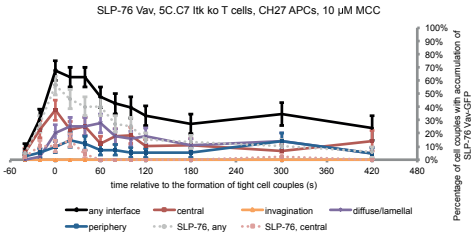


SLP-76 V3, 5C.C7 T cells, anti-B7, CH27 APCs, 10μM MCC

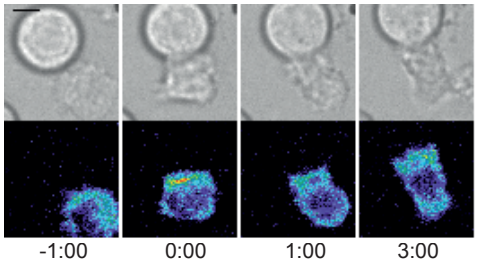


SLP-76 Vav, 5C.C7 T cells, anti-B7, CH27 APCs, 10μM MCC

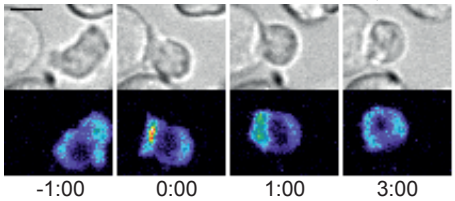


### Costimulation blockade

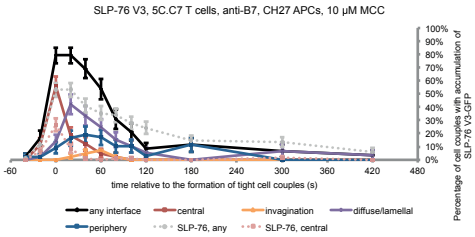


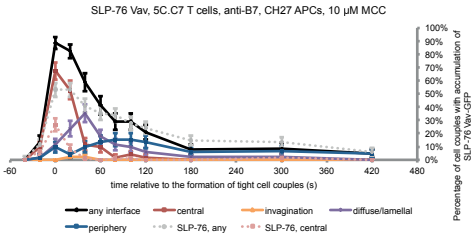


### Itk ko, costimulation blockade

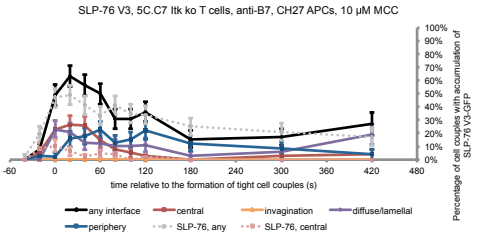


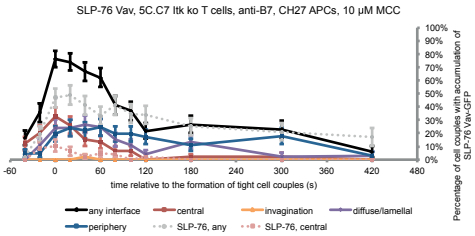


## B

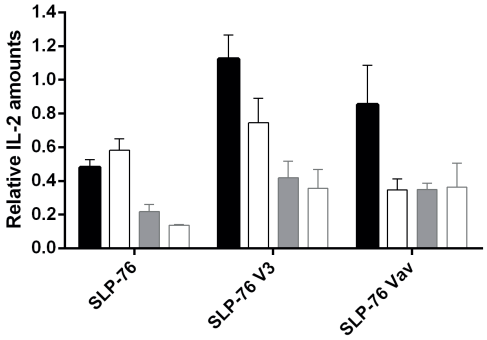


- full stimulus
- Itk ko, full stimulus
- costimulation blockade
- Itk ko, costimulation blockade

Statistical significance of differences in relative IL-2 mRNA

| Comparison | | SLP-76 | SLP-76 V3 | SLP-76 Vav |
|---|---|---|---|---|
| SLP76, full stimulus | Full stimulus | | 0.01 | |

**Figure 7**

**A**

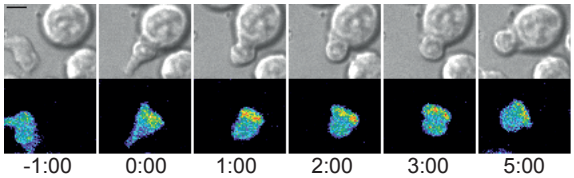


**B**

Full stimulus

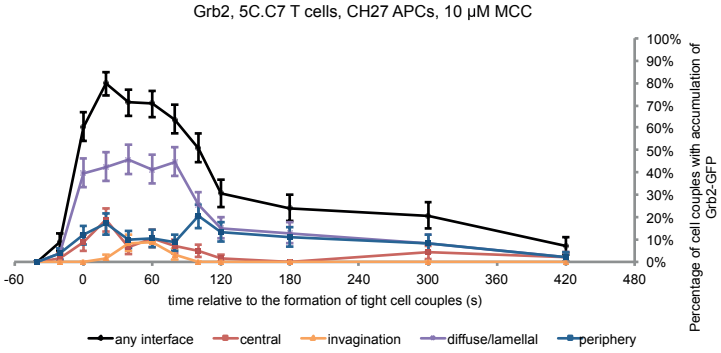


Itk ko, full stimulus

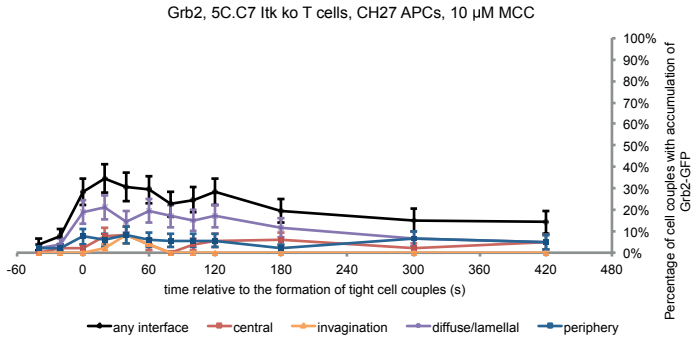


Costimulation blockade

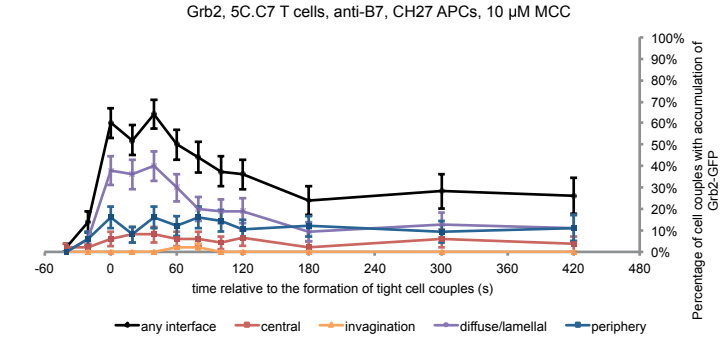


Itk ko, costimulation blockade

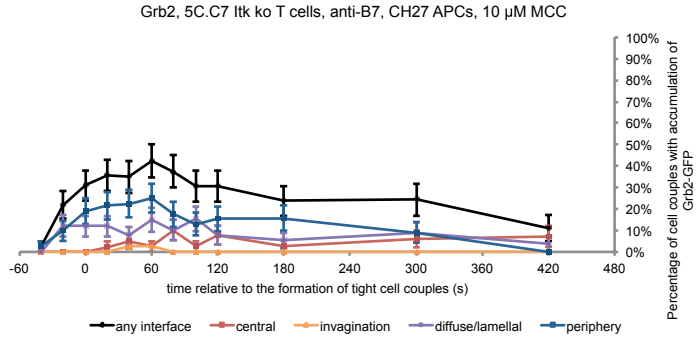

# Figure 8

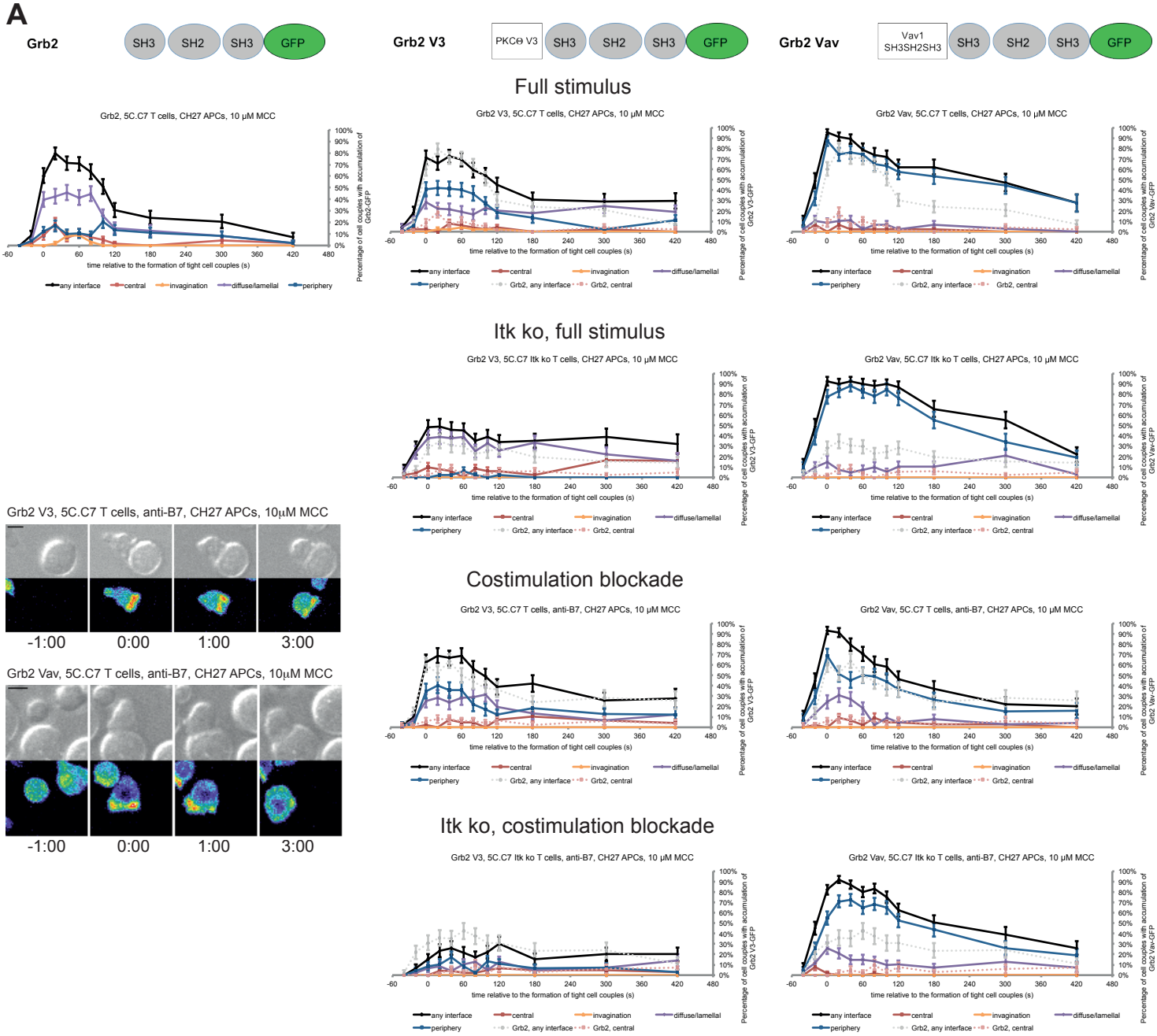


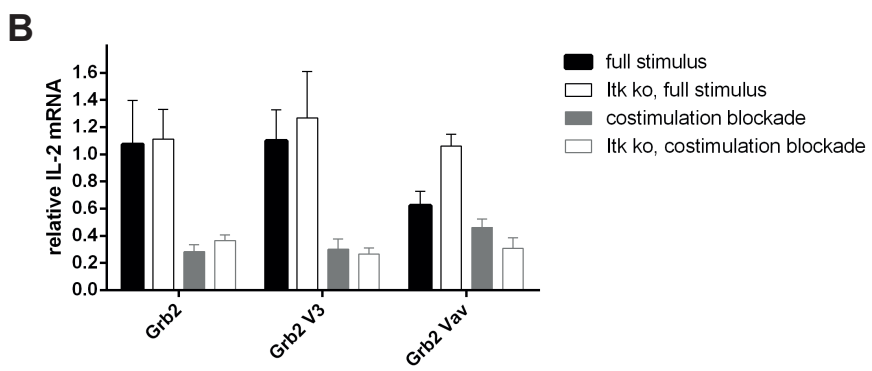


Statistical significance of differences in relative IL-2 mRNA

| | Comparison | Grb2 | Grb2 V3 | Grb2 Vav |
|---|---|---|---|---|
| Grb2, full stimulus | anti-B7 | 0.006 | 0.002 | |